Predicting Stability of DNA Duplexes in Solutions Containing Magnesium and Monovalent Cations

Richard Owczarzy,* Bernardo G. Moreira, Yong You, Mark A. Behlke, and Joseph A. Walder

Integrated DNA Technologies, 1710 Commercial Park, Coralville, Iowa 52241

Received November 30, 2007; Revised Manuscript Received March 8, 2008

ABSTRACT: Accurate predictions of DNA stability in physiological and enzyme buffers are important for the design of many biological and biochemical assays. We therefore investigated the effects of magnesium, potassium, sodium, Tris ions, and deoxynucleoside triphosphates on melting profiles of duplex DNA oligomers and collected large melting data sets. An empirical correction function was developed that predicts melting temperatures, transition enthalpies, entropies, and free energies in buffers containing magnesium and monovalent cations. The new correction function significantly improves the accuracy of predictions and accounts for ion concentration, G-C base pair content, and length of the oligonucleotides. The competitive effects of potassium and magnesium ions were characterized. If the concentration ratio of $[Mg^{2+}]^{0.5}/[Mon^+]$ is less than 0.22 $M^{-1/2}$, monovalent ions (K^+, Na^+) are dominant. Effects of magnesium ions dominate and determine duplex stability at higher ratios. Typical reaction conditions for PCR and DNA sequencing (1.5−5 mM magnesium and 20−100 mM monovalent cations) fall within this range. Conditions were identified where monovalent and divalent cations compete and their stability effects are more complex. When duplexes denature, some of the Mg^{2+} ions associated with the DNA are released. The number of released magnesium ions per phosphate charge is sequence dependent and decreases surprisingly with increasing oligonucleotide length.

Interactions of magnesium, sodium and potassium ions with DNA[1] and RNA molecules are important for essential functions of living cells and for molecular biology applications. Both divalent and monovalent cations bind to nucleic acid molecules and affect their physical properties (*1*). Magnesium cations stabilize nucleic acid duplexes and facilitate their folding into secondary and tertiary structures (*2*), which are biologically active. Mg^{2+} ions are also necessary cofactors of many enzymatic reactions involving nucleic acids (*3*). The total magnesium concentrations in various cells range from 5 to 30 mM; however, free Mg^{2+} concentrations are tightly controlled between 0.4 and 1.2 mM (*4*). Binding of monovalent cations also increases duplex stability. The major intracellular monovalent cation is K^+, while the major monovalent cation in extracellular fluid is Na^+.

Several theoretical models have been proposed to describe the complex phenomena of associations between cations and nucleic acids. The most widely used approaches are the mean-field approximation of the Poisson−Boltzmann equation (*5*−*8*), the counterion condensation model (*9, 10*), and Monte Carlo simulations (*11, 12*). There have been few experimental studies addressing effects of Mg^{2+} ion on the stability of short DNA duplexes (*13*−*16*), and comprehensive experimental melting data are not available. The majority of melting studies in magnesium buffers investigated genomic DNAs (e.g., calf thymus) (*5, 17*−*19*), long polymeric repeats (*20*−*22*), or biologically active RNA molecules (*2, 23*). Pioneering experiments done over 40 years ago (*17, 24*) showed that magnesium ions stabilize DNA duplexes significantly more than the same concentrations of monovalent ions. For example, 10 mM Mg^{2+} stabilizes a six base pair duplex nearly as much as a 1 M Na^+ solution (*13*), which is substantially more than what would be expected from the magnesium ion contribution to the ionic strength of the solution.

Numerous methods in molecular biology today (such as the polymerase chain reaction (PCR) and automated DNA sequencing) rely upon enzymatic reactions performed in the presence of Mg^{2+}. Most commonly, these buffers contain a mixture of monovalent cations (20−100 mM) and magnesium ions (1.5−5 mM). Specifically, PCR is usually done in buffers containing a mixture of magnesium chloride, tris(hydroxymethyl)aminomethane (Tris), deoxynucleoside triphosphates (dNTP), and KCl (*3*). Magnesium concentration is the critical parameter that influences both the efficiency and specificity of PCR (*25*−*29*), especially when total genomic DNA is used, long products are synthesized, or multiplex reactions are run. Low magnesium concentrations decrease the efficiency and yield of PCR. High Mg^{2+} concentrations increase the stability of primer−template duplexes and the efficiency of amplification; however, specificity is reduced because primers may anneal to incorrect template sites and unwanted sequences are more likely to

* To whom correspondence should be addressed. Telephone: +1 319 626-8459. Fax: +1 319 626- 9621. E-mail: science@owczarzy.net.

[1] Abbreviations: CE, capillary electrophoresis; DNA, deoxyribonucleic acid; dNTP, deoxynucleoside triphosphates; DSC, differential scanning calorimetry; EDTA, ethylenediaminetetraacetic acid; MOPS, 3-(*N*-morpholino)-propanesulfonic acid; NIST, National Institute of Standards and Technology; PCR, polymerase chain reaction; RNA, ribonucleic acid; SVD, singular value decomposition; TBI, tightly bound ion model; Tris, tris(hydroxymethyl)aminomethane; UV, ultraviolet.

10.1021/bi702363u CCC: $40.75
Published on Web 04/19/2008

be amplified (*27*). The optimal annealing temperature is 2−5 °C below the melting temperatures of primer−template duplexes (*26*). It is therefore desirable to predict melting temperatures accurately when PCR assays are designed.

Melting temperatures are usually predicted using the nearest-neighbor model with parameters determined for 1 M Na^+ buffer (*30, 31*). Since biological assays are implemented in various salt conditions, melting temperatures must be "corrected" for the presence and concentrations of all ions. Several empirical equations that correct T_m values in the presence of both Mg^{2+} and Na^+ ions have been suggested (*7, 15, 16, 32*), which are reviewed in the Results section. Our analysis demonstrated that use of these equations can lead to large errors in the predicted value of T_m (>10 °C). Better methods are needed to facilitate design of molecular biology experiments. We conducted a large set of UV melting experiments in solutions containing magnesium and monovalent (K^+, $Tris^+$, Na^+) ions to develop improved T_m magnesium correction methods. These experiments explored a wide range of magnesium and potassium ion concentrations under well-controlled conditions. Important physiologically relevant concentrations (1−10 mM Mg^{2+}, 50−200 mM KCl) were included. Novel, more accurate empirical formulas are presented that enable reliable T_m predictions in buffers containing dNTPs, magnesium, and monovalent ions.

MATERIALS AND METHODS

DNA Oligonucleotides. This work employed the same sets of DNA oligomers which were used in a previous study that explored the effects of sodium cations on T_m (*33*). All oligonucleotides were purified by denaturing polyacrylamide gel electrophoresis. Each single strand had an OH group on the 5′-end as well as on the 3′-end. All oligonucleotide samples passed two quality control tests. Capillary electrophoresis analysis (*33*) showed that oligonucleotides were at least 92% pure. Mass spectrometry using an Oligo HTCS system (Novatia, Princeton, NJ) confirmed DNA identity and purity. Experimentally measured molecular masses of all oligodeoxyribonucleotides deviated less than 3 g/mol from expected molecular masses.

UV Melting Studies. Typical PCR buffers contain 1.5 mM $MgCl_2$, 50 mM KCl, and 10 mM Tris-HCl (pH 8.3 at 25 °C). Studies of the pH effects on T_m were conducted in buffers where Tris was replaced with 10 mM potassium cacodylate for pH range from 6.5 to 7.7. The pH 8.3 buffer contained 10 mM 3-(*N*-morpholino)-propanesulfonic acid, MOPS. A combination glass electrode (Cat. No. 476306, Corning Inc., Corning, NY) with a Corning pH meter 240 was used to measure pH values. The electrode signal was compensated for temperature changes, which were measured by an ATC probe connected to the pH meter.

The effects of magnesium ions on T_m were examined in various buffers containing 10 mM Tris-HCl, 0−600 mM $MgCl_2$, and 0−1 M KCl. The pH was adjusted to 8.3 ± 0.03 with 0.1 M HCl at 25 °C. Buffers without KCl contained the lowest concentrations of Tris that were found to have sufficient buffering capacity, so that the pH of solutions at 25 °C before and after melting experiments did not differ by more than 0.1 unit. Specifically, 2 mM Tris was used for 0.5−20 mM magnesium buffers and 10 mM Tris was necessary for solutions of higher magnesium concentrations. Magnesium chloride was added from a 200 mM stock solution, because solid $MgCl_2$ is very hygroscopic and cannot be accurately estimated by weight. A complexometric assay (*34*) was employed to verify Mg^{2+} concentrations in each lot of the buffer. EDTA titrations showed that magnesium concentrations deviated less than 2% from expected values.

DNA concentrations were determined from absorbance (*33*). Complementary single-strands were mixed in a 1:1 molar ratio. Duplexes were desalted by dialysis against water in a 28-well microdialysis system (Invitrogen, Carlsbad, California), aliquoted based on solution weight, lyophilized in a Speed-Vac concentrator, rehydrated in magnesium melting buffers, and stored in −20 °C. Total single strand concentrations, C_t, were 2 ± 0.2 μM and were verified from recorded melting curves using absorbances of upper baselines. Several DNA duplexes were also dialyzed directly against magnesium buffers to check whether the desalting method led to complete exchange of the buffers. Since melting profiles of the same DNA sequences were superimposable, we can conclude that the desalting method exchanges melting buffers as effectively as direct dialysis against a melting buffer.

Melting experiments were conducted on a single beam Beckman DU 650 spectrophotometer with a Micro Tm Analysis accessory, a Beckman High Performance Peltier Controller, and 1 cm path length quartz cuvettes (Beckman Coulter, Fullerton, CA). Spectrophotometer software was modified to improve resolution and to more finely control rate of temperature changes (*33*). Both denaturation and renaturation transition curves were collected, and temperature was increased linearly at a rate of 24.9 ± 0.3 °C/h. Absorbance values at 268 nm were recorded every 0.1 °C. We employed Beckman cuvettes (Cat. No. 523880) wherein the top was sealed with a Teflon stopper to prevent evaporation. These cuvettes are small (~330 μL) and have thin walls, so heat is quickly distributed and the cuvettes are easily equilibrated to desired temperatures. Accuracy of temperature measurements inside of the cuvettes was validated using an external probe with a thermistor thermometer 874C (Tegam, Inc.). The thermistor (type K) was calibrated using a NIST traceable mercury thermometer of 0.1 °C resolution when both thermometers measured temperatures of both boiling water and ice−water mixture. Temperature values reported by the spectrophotometer were found to agree with the temperature values reported by the thermistor within 0.5 °C throughout the range from 15 to 97 °C.

Melting experiments were analyzed using previously published procedures (*30, 33*). Melting curves of buffers alone were subtracted from raw DNA melting curves. Regions of linear increase of absorbance before and after the melting transition were least-squares fitted to lower and upper linear baselines, and the fraction of broken base pairs, θ, was calculated as described previously (*33*). All melting curves showed a single, S-shaped transition for all buffers studied, allowing T_m to be unambiguously determined (see Figure S1 of the Supporting Information). Both upper and lower linear baselines were well established even when the melting temperatures were above 80 °C. In such cases, absorbance values were collected up to 99 °C. Melting profiles were smoothed and T_m values were determined (*35*) as temperatures where $\theta = 0.5$. Three to eight melting profiles were acquired for each DNA sample in two different

cuvettes, and their T_m values were averaged. The average standard deviation of UV experimental melting temperatures, σ_{Tm}, was estimated to be 0.3 °C.

Differential Scanning Calorimetry (DSC). Experiments were conducted using a Nano II differential scanning calorimeter (Calorimetry Sciences Corporation, American Fork, UT) and a 60 base pair long DNA duplex, 5′-TTC GCG GAT TAG CCC TAC GCA TCG GTT ACA AAC GAG GAC CTT ATG CAC TTT GAC AGC ATG-3′. Samples were degassed for 17 min at 25 mmHg vacuum. Buffer scans were subtracted from DNA scans (*33*). The total single strand concentration was 2 μM. Melting temperatures at the maxima of the excess heat capacity curve, T_m(DSC), were reproducible within 0.3 °C.

Statistical Analysis of T_m Predictions. To critically evaluate the accuracy of T_m magnesium corrections, average errors of T_m predictions, $\langle|\Delta T_m|\rangle_{AV}$, and reduced χ_r^2 values were calculated for each T_m magnesium correction function. Experimentally observed melting temperatures, T_m(experiment,i), were compared with predicted melting temperatures, T_m(prediction,i), for a set of n measurements,

$$\langle|\Delta T_m|\rangle_{AV} = \frac{\sum_{i=1}^{n} |T_m(\text{prediction}, i) - T_m(\text{experiment}, i)|}{n} \quad (1)$$

$$\chi_r^2 = \frac{1}{\nu}\left[\frac{\sum_{i=1}^{n} (T_m(\text{prediction}, i) - T_m(\text{experiment}, i))^2}{\sigma_{Tm}^2}\right] \quad (2)$$

where $|T_m(\text{prediction},i) - T_m(\text{experiment},i)|$ is the absolute value of the difference between predicted and experimentally measured melting temperatures and ν is the number of degrees of freedom. F-tests (*36, 37*) were conducted to determine the goodness-of-fit and accuracy of T_m predictions. The χ_r^2 values were compared between different T_m magnesium correction functions. A smaller χ_r^2 value reflects a better ability of the model to describe experimental results. Probabilities, P, of the null hypothesis that observed differences in χ_r^2 values were insignificant and could happen by random chance alone were evaluated. The smaller the P value is, the more significant the difference is between two magnesium corrections. If the P value was less than 0.05, the null hypothesis was rejected and the differences in goodness-of-fit were considered to be statistically significant. This analysis assumed that errors of melting data were normally distributed and was implemented using the Excel FDIST function.

RESULTS

Effects of Buffer pH on Melting Temperature. Phosphate, cacodylate or citrate buffers are commonly used in DNA melting experiments. In this study, we wished to characterize melting behavior in buffers that are used in biological applications. We therefore employed Tris buffer, since this is the most widely used buffer in molecular biology applications, including PCR. The pH values of Tris buffers decrease with increasing temperature. This change is rather large in comparison with other biological buffers (*38, 39*). Since DNA contains several groups capable of deprotonation and protonation, questions arise about pH changes during PCR and their effects on duplex stability. We therefore measured the pH of a typical PCR buffer (1.5 mM $MgCl_2$, 50 mM KCl and 10 mM Tris-HCl, pH = 8.3 at 25 °C) when the temperature was increased from 10 to 90 °C. The pH was found to be a linear function of temperature with a d(pH)/dT coefficient of -0.020 K^{-1} (data not shown). To examine effects of changes in pH on melting temperatures, the same DNA duplexes were melted in the PCR buffer and in buffers where Tris was replaced with either 10 mM potassium cacodylate or 10 mM MOPS (see Materials and Methods). These two compounds manifest a much lower dependence of pK_a on temperature than Tris; the published values of d(pH)/dT are 0.0019 K^{-1} and -0.011 K^{-1} for cacodylic acid and MOPS, respectively (*39, 40*).

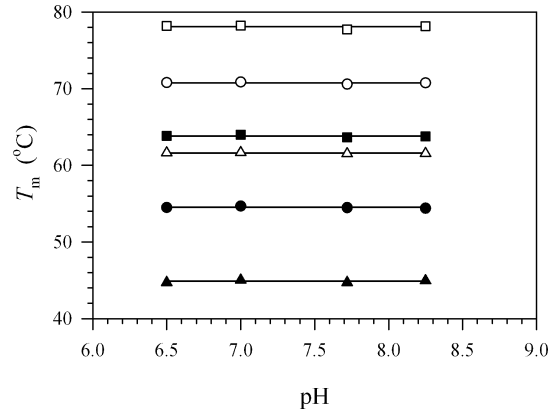

FIGURE 1: Melting temperatures of DNA duplex oligomers are independent of pH in the range from 6.5 to 8.3. Solid symbols are 15-mers, open symbols are 30-mers, fraction of G·C base pairs vary from 0.3 to 0.7. Sequences are TTCTACCTATGTGAT (solid triangle), GCAGTGGATGTGAGA (solid circle), CAGCCTCGTCGCAGC (solid square), CTTAAGATATGAGAACTTCAACTAATGTGT (open triangle), AGTCTGGTCTGGATCTGAGAACTTCAGGCT (open circle), GACCTGACGTGGACCGCTCCTGGGCGTGGT (open square). Buffers contained 1.5 mM $MgCl_2$, 50 mM KCl and 10 mM cacodylic acid or MOPS.

Figure 1 shows DNA melting temperatures in cacodylate and MOPS buffers of various pH. Twelve DNA oligomers ranging in length from 15 to 30 base pairs and in fraction of G·C base pairs, f_{GC}, from 0.3 to 0.7 were studied. Melting temperatures in environments of pH from 6.5 to 8.3 varied less than 0.5 °C. T_m values were found to be independent of pH and in agreement with T_m values observed in the PCR buffer that was prepared from Tris. Although the pH of the PCR Tris buffer decreased from 8.3 to 6.9 when temperature increased from 25 to 95 °C, the resulting pH changes had insignificant effects on melting temperatures of native duplex DNAs. This result is consistent with previous studies where melting temperatures of a DNA hairpin (*41*), T_2 phage DNA (*42*), and calf thymus DNA (*43*) did not change significantly in the range of pH values from 6.5 to 8.0.

Comparison of DNA Duplex Stability in Na^+ and K^+ buffers. Since PCR buffers typically contain potassium and Tris ions, it is of interest to compare the stabilizing effects of these monovalent ions with sodium ions. Nakano et al. (*14*) found in the study of a single DNA duplex, d(GCCAGTTAA), that the effects of Na^+ and K^+ on T_m were equivalent. However, we recently discovered that the influence of sodium ions on duplex stability is far more complex than previously thought (*33*). The stabilizing effect is sequence dependent and cannot be described by a simple

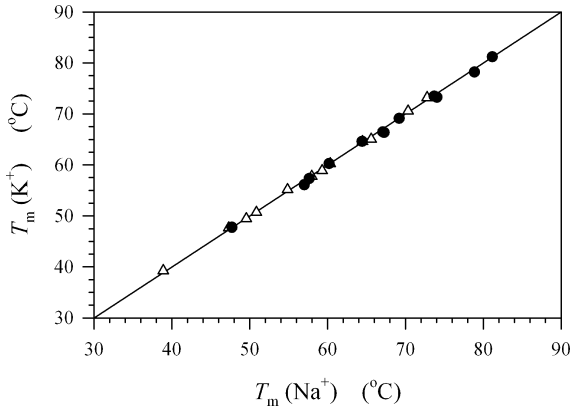

FIGURE 2: Comparison of effects of Na^+ and K^+ on melting temperatures in buffers of 55 mM (open triangle) and 205 mM (closed circle) monovalent ion concentrations. Duplex sequences ($C_t = 2\ \mu M$) are in Table 4. Oligonucleotide lengths range from 15 to 30 base pairs. Melting temperatures determined in 10 mM Tris-HCl and 50 or 200 mM KCl buffers are plotted versus melting temperatures measured in 10 mM sodium phosphate and NaCl buffers (*33*). Diagonal solid line connects points where melting temperatures in both buffers would be the same.

linear relationship with respect to ln [Na^+]. We therefore examined a larger set of duplexes to compare the effects of sodium and potassium cations.

Twelve DNA duplexes were melted in buffers containing 10 mM Tris and KCl of various concentrations ranging from 50 mM to 1 M as well as in sodium buffers (*33*). The stabilizing effect of K^+ ions is also sequence dependent, and the dependence of $1/T_m$ on ln [K^+] is nonlinear. Comparison of melting temperatures is shown in Figure 2. Differences between T_m values measured in sodium and potassium solutions of the same concentrations are within experimental errors. The best T_m agreement is achieved when Tris ions are taken into account. About half of the Tris molecules are protonated in the PCR buffer, i.e., 10 mM Tris buffer adds approximately 5 mM to the total monovalent ion concentration, [Mon^+]. In summary, K^+, Na^+, $Tris^+$ ions stabilize DNA duplexes with similar potency, and their effects on duplex stability are additive,

$$[Mon^+] = [K^+] + [Tris^+] + [Na^+] \quad (3)$$

The published T_m correction formula for sodium ions (*33*) is therefore also applicable to buffers containing Tris or KCl,

$$\frac{1}{T_m(Mon^+)} = \frac{1}{T_m(1\ M\ Na^+)} + (4.29 f_{GC} - 3.95) \times 10^{-5} \ln[Mon^+] + 9.40 \times 10^{-6} (\ln[Mon^+])^2 \quad (4)$$

where $T_m(Mon^+)$ is the melting temperature in the buffer containing a mixture of monovalent ions and T_m(1 M Na^+) is the melting temperature in reference 1 M Na^+ buffer. Equations 3 and 4 may be less accurate in high concentrations (above 100 mM) of monovalent ions capable to form hydrogen bonds (ammonium, Tris) and for bulkier monovalent ions (tetramethylammonium). Affinity of these ions to DNA has been reported to differ slightly from the affinity of Na^+ and K^+ (*67, 68*). We have not investigated the bulkier monovalent ions under such conditions.

Previously Published T_m Magnesium Corrections. The nearest-neighbor model and thermodynamic parameters (*30, 31, 66*) provide accurate predictions of duplex stability in 1 M Na^+ buffer from DNA sequence and oligonucleotide concentration. To predict melting temperatures in magnesium buffers, $T_m(Mg^{2+})$, a correction function that scales melting temperatures from the reference 1 M Na^+ buffer to the magnesium buffer is applied. Although magnesium ions stabilize duplexes significantly more than the same concentration of sodium ions (*13, 17*), previously published T_m correction formulas generally assume that the stabilizing effects of magnesium ions are qualitatively similar to the better characterized stabilizing effects of sodium ions. These formulas use the T_m salt correction for sodium ions to predict duplex stability in Mg^{2+} solutions using a simple adjustment wherein Mg^{2+} ion concentration is converted to an "equivalent" Na^+ concentration, [Na^+_{eq}], which is then directly used in the T_m sodium salt correction. The "equivalent" Na^+ concentration is defined as the concentration of sodium ions in a buffer that stabilizes duplexes to the same extent as the magnesium buffer. The following formula was suggested,

$$[Na^+_{eq}] = \beta\sqrt{[Mg^{2+}]} + [Mon^+] \quad (5)$$

where concentrations are in mol/L (*15, 16, 32*). Effects of magnesium and monovalent ions are assumed to be additive in eq 5. The total concentration of monovalent ions, [Mon^+], is the sum of concentrations of alkali metal and amine cations (Na^+, K^+, $Tris^+$). Values from 3.3 to 4.0 have been used for the parameter β (*15, 16, 32*). The equivalent [Na^+_{eq}] values are entered into the T_m corrections for sodium salts (*31, 45*) to correct melting temperatures for magnesium solutions. Peyret used this concept and proposed the following empirical correction in his doctoral dissertation (*16*) where the salt dependence was presumed to be entirely entropic:

$$\frac{1}{T_m(Mg^{2+})} = \frac{1}{T_m(1\ M\ Na^+)} + \frac{0.368(N_{bp} - 1)}{\Delta H^\circ} \times \ln\left(3.3 \times \sqrt{[Mg^{2+}]} + [Mon^+]\right) \quad (6)$$

N_{bp} is the number of base pairs in the duplex, and ΔH° is the standard enthalpy of duplex annealing (cal/mol) that can be measured experimentally or estimated from nearest-neighbor parameters (*31, 66*). T_m values have units of kelvins. The term $N_{bp} - 1$ is relevant for synthetic oligonucleotides and reflects the number of phosphate groups in the duplex divided by 2 (*31*). The melting data used to develop eq 6 have not been published, and the accuracy of T_m predictions using this method has not been established.

Ahsen et al. (*15*) compiled a set of melting temperatures for 162 probes determined using a real-time PCR LightCycler system. Either the probes were dye-labeled or buffers contained SYBR Green I. A revised version of eq 6 was proposed with a larger β value of the magnesium term,

$$\frac{1}{T_m(Mg^{2+})} = \frac{1}{T_m(1\ M\ Na^+)} + \frac{0.368(N_{bp} - 1)}{\Delta H^\circ} \times \ln\left(3.79\sqrt{[Mg^{2+}]} + [Mon^+]\right) \quad (7)$$

In their analysis, Ahsen et al. did not consider thermodynamic effects of fluorescent dyes and quenchers on DNA duplex stability, although these effects can be significant (*34*). The authors reported that their heating rates (0.1−0.2 °C/s) were probably too fast to achieve equilibrium conditions and T_ms may have been slightly overestimated. Even with these

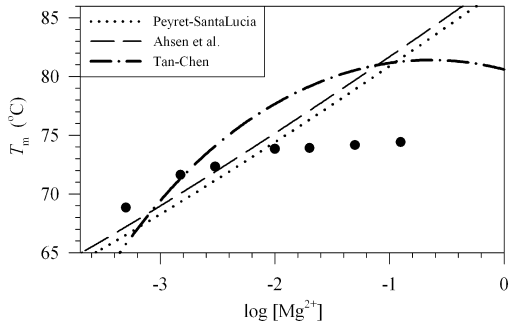

FIGURE 3: Comparison of some commonly used T_m magnesium correction functions. Experimentally measured (solid circle) and predicted melting temperatures for 30-mer duplex, ODN11, 5′-AGTCTGGTCTGGATCTGAGAACTTCAGGCT-3′ in buffers containing 10 mM Tris-HCl and various amounts of Mg^{2+} ions are shown.

limitations, the standard error of T_m predictions was 1.8 °C for perfectly matched duplexes (*15*).

Mitsuhashi (*32*) suggested an even larger value of β and combined eq 5 with an earlier T_m sodium correction function derived by Schildkraut and Lifson (*45*):

$$T_m(Mg^{2+}) = T_m(1\ M\ Na^+) + 16.6 \log\left(4\sqrt{[Mg^{2+}]} + [Mon^+]\right) \quad (8)$$

The accuracy of eq 8 was not reported. Equations 6−8 are routinely used for solutions containing magnesium ions in the presence, or absence, of other monovalent ions.

Recently, Tan and chen proposed the tightly bound ion model, TBI, which employs separate treatments for tightly bound ions and for diffuse ions surrounding DNA molecules (*7, 46*). The model accounts for discrete modes of counterion binding. Fluctuations and correlations between the ions tightly bound to DNA are considered, while these effects were neglected in previous models based solely on the mean-field approach of the Poisson−Boltzmann equation. The TBI model provides new practical formulas for thermodynamic parameters as a function of magnesium and sodium concentrations. For T_m, the following relationship is obtained:

$$\frac{1}{T_m(Mg^{2+}, Na^+)} = \frac{1}{T_m(1\ M\ Na^+)} - \frac{0.00322(N_{bp} - 1)}{\Delta H^\circ}(x_1\Delta g_1 + x_2\Delta g_2 + \Delta g_{12}) \quad (9)$$

where x_1 and x_2 are the fractional contributions of Na^+ and Mg^{2+} to the duplex stability and Δg_1 and Δg_2 are the mean electrostatic folding free energies per base stack in pure Na^+ or Mg^{2+} solutions (kcal/mol), respectively (*46*). The crossing term Δg_{12} accounts for interference and competition of Na^+ ions with Mg^{2+} counterions (e.g., $\Delta g_{12} = 0$ for pure magnesium solutions). Expression 9 was proposed to be appropriate for duplexes with six or more base pairs (*7, 46*).

To examine the validity of these previous models, we initially studied melting temperatures for several duplexes ranging from 10 to 30 base pairs in length. Magnesium concentrations varied from 0.5 mM to 125 mM in the presence of 10 mM Tris buffer with no Na^+ or K^+. Figure 3 illustrates results of predictions using eqs 6−9 starting from the experimentally measured T_m in 1 M Na^+ buffer for one such duplex. Predicted T_m values were found to deviate substantially from measured values over the entire range of magnesium concentrations. Qualitatively similar results were seen for the remaining sequences. Errors of greater than 10 °C in the predicted melting temperature were observed in some cases. Since the published T_m correction functions did not accurately predict melting temperatures, we proceeded to study systematically a larger data set and develop new equations to model T_m in the presence of Mg^{2+}.

Magnesium Ions and DNA Melting Temperatures. We first characterized the effects of magnesium ions on DNA duplex stability in a simple system where monovalent ions had negligible thermodynamic effects and magnesium ions were dominant. In this set of experiments, melting temperatures were measured in 0.5−600 mM Mg^{2+}. To maintain stable pH, 2 mM Tris was present for 0.5−20 mM Mg^{2+} solutions, and 10 mM Tris was used in the 50−600 mM Mg^{2+} buffers. No KCl was added. As shown later, effects of Tris ions on T_m are negligible under these conditions.

Table 1 illustrates sequences studied and trends in their melting temperatures. The remaining data are presented in Table S1 of the Supporting Information. The set consisted of 92 DNA duplex oligomers (*33*) ranging in f_{GC} from 0.2 to 0.8 and in the number of base pairs from 10 to 30. Oligonucleotides annealed into blunt-ended, non-self-complementary duplexes and were designed to avoid self-dimer, hairpin, or other competing structures. Circular dichroism spectra demonstrated that the secondary structure of DNA with Mg^{2+} as the counterion is similar to that with Na^+, throughout the range of magnesium concentrations used in biological assays (Figure S2 of the Supporting Information). However, subtle changes of secondary structure occur at high magnesium concentrations (>130 mM). Long regions of consecutive G·C or A·T base pairs were removed from sequences to decrease non-two-state melting behavior. All 10 internal nearest-neighbor doublets and 2 end (initiation) interactions were well represented, so that sequence dependent properties could be examined (*30, 44, 66*). Over 3000 UV melting profiles were collected. All melting curves showed a single, S-shaped transition (see Figure S1). Samples were deemed to be in thermodynamic equilibrium because their denaturation and renaturation melting profiles overlapped. No decreases of absorbance at 268 nm or increases of absorbance at 350 nm, which are characteristic of DNA aggregation or precipitation (*18, 19, 22*), were observed during melting transitions. Representative examples of the dependence of melting temperatures on ln [Mg^{2+}] are shown in Figure 4. The relationships are nonlinear functions of oligonucleotide length, G·C base pair content, and magnesium concentration. When Mg^{2+} is added to a solution of duplex DNAs, the melting temperature increases until a maximum is reached. Higher Mg^{2+} concentrations destabilize duplexes slightly. Figure 4 demonstrates that the peaks of maximum stability are wide. The magnesium concentration at which the maximal T_m value occurs is sequence dependent, varying from 25 mM to 350 mM Mg^{2+} for different duplexes in the data set. The maximum T_m shifts to a lower magnesium concentration the higher the fraction of G·C base pairs (see Figure S3 of the Supporting Information). As magnesium concentration is increased, stabilizing T_m effects are saturated first for G·C rich duplexes and later for A·T rich duplexes.

Since thermodynamic parameters and the nearest-neighbor model predict DNA stability in 1 M Na^+, we employed this

Table 1: Experimental Melting Temperatures for 18 DNA Duplex Oligomers in Buffers of a Wide Range of Magnesium Concentrations

DNA sequence (5′ to 3′)	T_m (°C) at [Mg^{2+}] indicated[a]								
	0.5 mM[b]	1.5 mM[b]	3.0 mM[b]	10 mM[b]	20 mM[b]	50 mM[c]	125 mM[c]	300 mM[c]	600 mM[c]
TTGTAGTCAT	27.2	30.9	32.3	34.9	36.0	37.3	37.5	37.1	35.4
ATCGTCTGGA	35.1	38.9	40.6	43.4	43.4	43.7	44.4	43.0	41.6
GATGCGCTCG	44.0	47.7	48.8	50.7	51.2	51.6	51.9	49.9	47.7
GGGACCGCCT	48.3	51.9	53.7	55.5	55.9	55.4	56.1	54.9	52.2
CGTACACATGC	40.2	44.2	45.7	48.1	48.0	48.1	48.6	47.0	44.9
CCATTGCTACC	38.9	42.7	44.2	46.3	46.9	47.2	47.5	47.0	44.8
TTCTACCTATGTGAT	43.3	46.1	47.8	50.2	50.4	51.0	51.5	50.7	49.4
GCAGTGGATGTGAGA	52.3	55.1	56.5	58.1	58.7	59.2	59.0	58.2	56.1
CAGCCTCGTCGCAGC	61.9	64.1	65.3	66.8	67.3	67.5	67.3	65.5	63.7
TGATTCTACCTATGTGATTT	51.8	54.6	55.8	57.7	58.2	59.3	59.5	58.8	57.7
AGCTGCAGTGGATGTGAGAA	61.1	63.7	64.8	66.3	66.8	67.7	67.3	66.3	64.7
CAGCCTCGTTCGCACAGCCC	68.9	71.3	72.3	73.4	73.9	74.2	73.9	72.3	70.3
GTTCTATACTCTTGAAGTTGATTAC	57.2	59.7	60.8	62.4	63.0	63.8	64.0	63.5	62.6
CTGGTCTGGATCTGAGAACTTCAGG	65.6	67.7	68.7	69.8	70.3	70.7	70.6	69.8	68.6
CAGTGGGCTCCTGGGCGTGCTGGTC	73.5	75.3	76.2	77.3	77.6	78.2	77.4	75.9	74.0
CTTAAGATATGAGAACTTCAACTAATGTGT	61.0	63.1	64.1	65.5	66.0	67.1	67.1	66.2	65.2
AGTCTGGTCTGGATCTGAGAACTTCAGGCT	69.8	71.6	72.5	73.6	73.9	74.2	74.4	73.5	72.2
GACCTGACGTGGACCGCTCCTGGGCGTGGT	76.1	77.8	78.6	79.4	79.7	80.0	79.8	78.1	76.4

[a] $C_t = 2 \pm 0.2$ μM. Buffers do not contain any KCl. [b] 2 mM Tris-HCl buffers. [c] 10 mM Tris-HCl buffers.

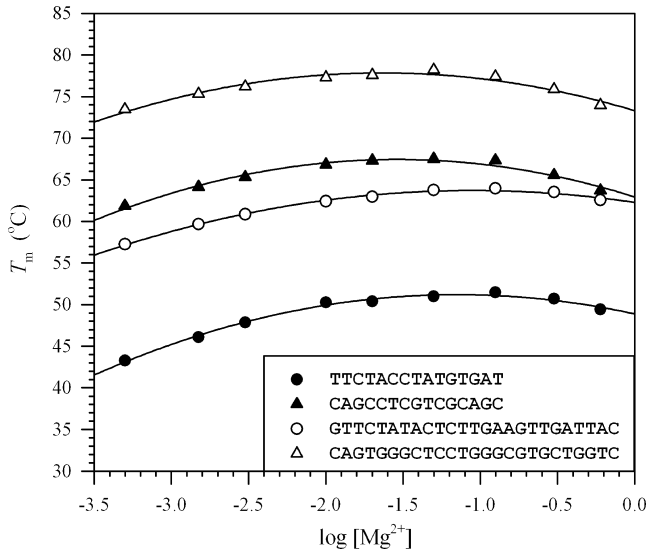

FIGURE 4: Dependence of melting temperatures on magnesium concentrations is plotted for representative duplexes, which are 15 (solid symbols) and 25 (open symbols) base pairs long. Percentages of G·C base pairs were either 32−33% (circle) or 72−73% (triangle). $Tris^+$ ions are present at low concentrations where they have negligible effects on duplex stability. Experimental data were fitted with quadratic curves to illustrate trends.

ionic environment as the reference salt concentration, as has been done in previous studies (*15, 16, 31, 33*). Differences between reciprocal T_m values in each magnesium buffer and 1 M Na^+ (*33*) were calculated. Figure 5 shows the dependence of these differences on f_{GC}, and N_{bp} present in the DNA duplexes. At fixed oligonucleotide length and constant magnesium concentration, the $1/T_m$ differences vary approximately linearly with f_{GC}:

$$\frac{1}{T_m(Mg^{2+})} - \frac{1}{T_m(1\ M\ Na^+)} = S_{GC} f_{GC} + Y_{GC} \qquad (10)$$

Deviations from linear relationships seen in Figure 5 are caused by experimental errors and by additional sequence-dependent effects (e.g., nearest-neighbor interactions). However, incorporation of nearest-neighbor parameters instead of a single term for f_{GC} did not significantly improve the accuracy of the T_m correction (Supporting Information, Table S5). Similarly, attempts to develop nearest-neighbor parameters for the effect of monovalent ions did not improve the accuracy of the T_m salt correction for sodium ions (*33*). The slopes S_{GC} are negative in buffers of low magnesium concentration (Figure 5A,B) and increase with increasing magnesium concentration. The fitted lines become flat at about 14 mM Mg^{2+} where the difference $1/T_m(Mg^{2+}) - 1/T_m(1\ M\ Na^+)$ is independent of the fraction of G·C base pairs. In buffers having higher Mg^{2+} concentrations, the slopes are positive (Figure 5D).

In comparison with experimental errors, differences in the slopes were minor. In order to simplify fitting of the data, we averaged S_{GC} slopes at each magnesium concentration. Averages were weighted based on the number of oligonucleotides of given length. These weight-averaged S_{GC} values are plotted versus the natural logarithm of magnesium concentration in Figure 6A. A linear relationship is observed ($r^2 = 0.993$):

$$S_{GC} = c + d \ln[Mg^{2+}] \qquad (11)$$

where the fitted parameters c and d are equal to 6.47×10^{-5} and 1.46×10^{-5} K^{-1}, respectively ([Mg^{2+}] is in mol/L). Substitution of eq 11 into eq 10 allows us to calculate intercepts Y_{GC}:

$$Y_{GC} = \frac{1}{T_m(Mg^{2+})} - \frac{1}{T_m(1\ M\ Na^+)} - f_{GC}(6.47\times10^{-5} + 1.46\times10^{-5} \ln[Mg^{2+}]) \qquad (12)$$

Figure 5 shows that Y_{GC} values change with N_{bp} and hence the number of negatively charged phosphate groups, Z, and seem to approach a limiting value with increasing duplex length. Since our chemically synthesized DNA duplexes do not contain phosphate groups on the 3′ or 5′ termini, Z is equal to $2(N_{bp} - 1)$. In Figure 6B, values of Y_{GC} calculated from eq 12 and averaged for each oligomer length are plotted versus $1/[2(N_{bp} - 1)]$. Linear relationships are observed, so Y_{GC} can be described by the following equation:

$$Y_{GC} = S_{Nbp} \frac{1}{2(N_{bp} - 1)} + I_{Nbp} \qquad (13)$$

where the slope S_{Nbp} and intercept I_{Nbp} vary with magnesium

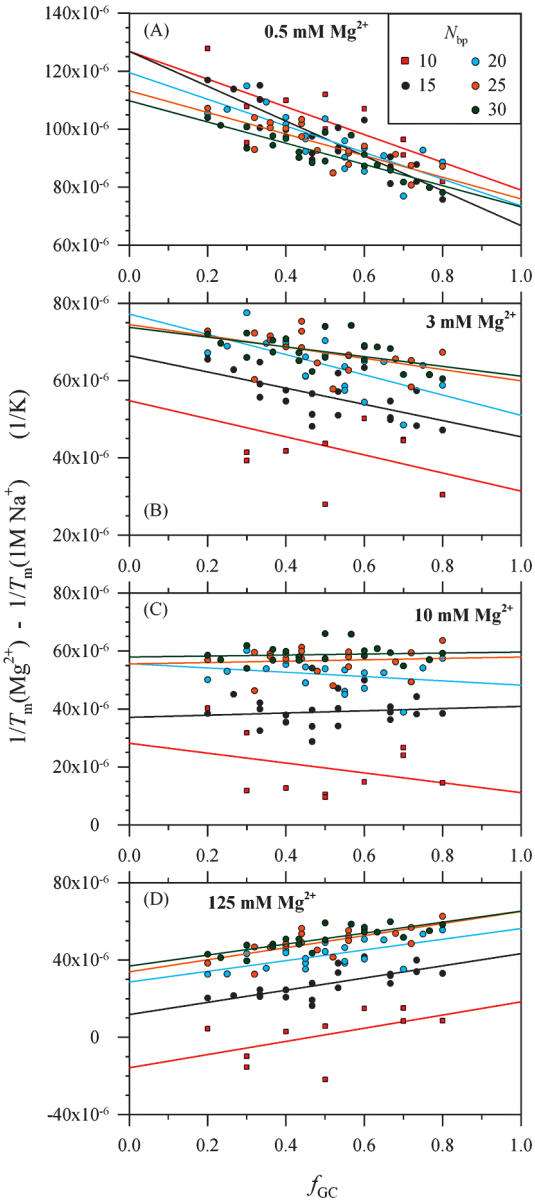

FIGURE 5: Differences between $1/T_m$ values in buffers of various Mg^{2+} concentrations and 1 M Na^+ buffer are shown as a function of f_{GC}. Inset shows colored symbols used for oligonucleotides of various lengths. (A) 0.5 mM Mg^{2+}, (B) 3 mM Mg^{2+}, (C) 10 mM Mg^{2+}, (D) 125 mM Mg^{2+}.

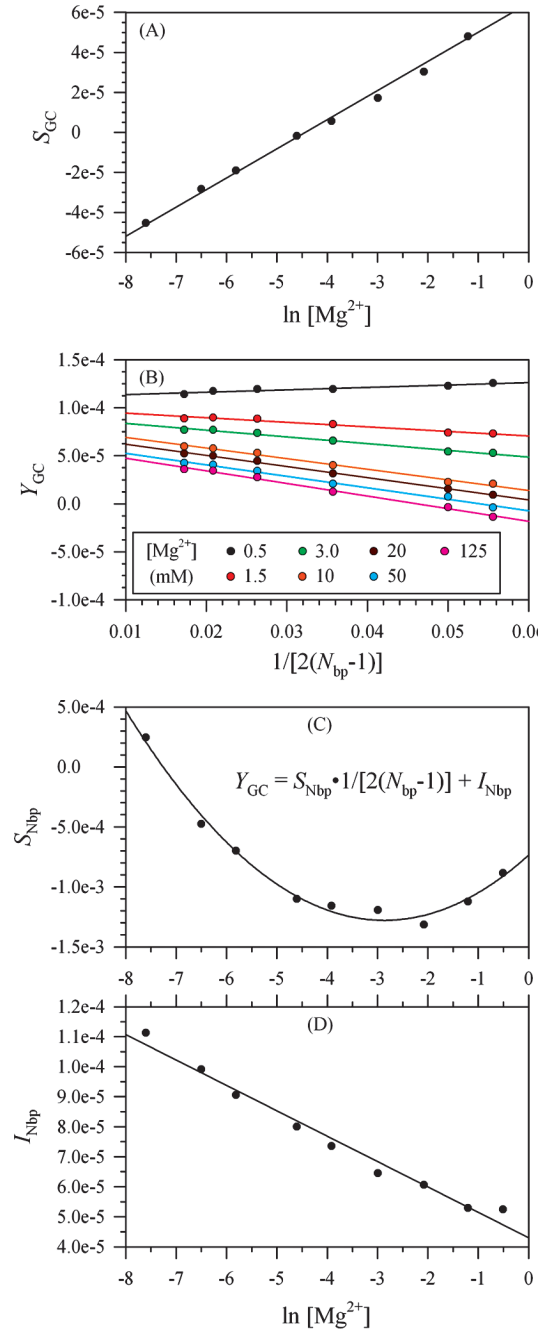

FIGURE 6: Slopes (A) and intercepts (B) of fitted straight lines from Figure 5 are examined. Panels (C) and (D) display dependence of slopes and intercepts of fitted straight lines from Figure 6B on Mg^{2+} concentrations.

concentration. Figure 6C and Figure 6D show that these relationships can be approximated as

$$I_{Nbp} = a + b \ln[Mg^{2+}] \quad (14)$$

$$S_{Nbp} = e + f \ln[Mg^{2+}] + g(\ln[Mg^{2+}])^2 \quad (15)$$

where a, b, e, f, and g are empirical parameters.

Combination of eqs 10, 11, and 13−15 yields the T_m magnesium correction,

$$\frac{1}{T_m(Mg^{2+})} = \frac{1}{T_m(1\ M\ Na^+)} + a + b \ln[Mg^{2+}] + f_{GC}(c + d \ln[Mg^{2+}]) + \frac{1}{2(N_{bp}-1)}[e + f \ln[Mg^{2+}] + g(\ln[Mg^{2+}])^2] \quad (16)$$

This equation can be used to scale melting temperatures of DNA duplex oligomers to different magnesium buffers when DNA concentration is fixed.

Stepwise fits allowed us to develop eq 16; however, the parameters obtained from these consecutive fits are not optimal because experimental data are not weighted equally. We therefore applied multivariate linear regression and fitted the seven parameters of eq 16 (a, b, c, d, e, f, g) in one step. The experimental data set consisted of 680 T_m values for 92 unique duplex DNAs measured in various Mg^{2+} concentrations (Tables 1 and S1). The set of empirically derived parameters and their errors are presented in Table 2. Extra significant figures of the parameters are included to prevent rounding errors. The multivariate fits were calculated using the Excel LINEST function as well as the numerically stable

Table 2: Parameters Obtained Using the Multivariate Fit to Eq 16 in Reciprocal Kelvins

parameter	value (K^{-1})	standard error (K^{-1})
a	3.92×10^{-5}	0.2×10^{-5}
b	-9.11×10^{-6}	0.5×10^{-6}
c	6.26×10^{-5}	0.4×10^{-5}
d	1.42×10^{-5}	0.08×10^{-5}
e	-4.82×10^{-4}	0.7×10^{-4}
f	5.25×10^{-4}	0.2×10^{-4}
g	8.31×10^{-5}	0.2×10^{-5}

REGRL function (Matrix and Linear Algebra for Excel v.1.8.1, Foxes team, Roma, Italy, http://digilander.libero.it/foxes). Both functions gave identical results. Errors were estimated from residuals of the fit and from bootstrap simulations (*47*). The bootstrap estimates of the standard errors were up to 35% higher than errors from the residuals of multivariate regression and serve as a liberal estimate of the parameter errors reported in the third column of Table 2. Ten thousand bootstrap sample data sets were generated using Microsoft Excel. Each bootstrap data set was of the same size (680 T_m's) and was constructed by random drawing of T_m values, with replacement, from the original experimental data set. In other words, the entire experimental data set was used in each drawing. The parameters (*a*, *b*, *c*, *d*, *e*, *f*, *g*) were obtained from each bootstrap data set using the multivariate fit. Averages of bootstrap parameters agreed with values calculated from the original experimental data set. Standard deviation of each parameter was estimated from ten thousand bootstrap parameters (*47*).

Singular value decomposition (SVD) was employed to examine fits and correlations between parameters (*37*). The rank of the SVD design matrix was seven for the experimental and bootstrap data sets. Therefore, the seven fitted parameters were unique, i.e., none of the parameters could be obtained from linear combinations of the remaining parameters. An F-test was carried out to evaluate the significance of each of the parameters. The probability was estimated whether improvements in χ_r^2 could happen by random chance alone when the parameter and its term are added to the remaining 6 parameters (*36*). The null hypothesis assumed that the parameter does not improve fit and does not decrease χ_r^2 significantly. Since the probabilities were less than 10^{-18} for all parameters, the null hypotheses were rejected and each of the seven parameters in eq 16 was found to be statistically significant. If any single parameter is neglected, the accuracy of the T_m predictions declines.

It is important to assess the accuracy of T_m predictions obtained from eq 16. Figure S4 of the Supporting Information shows errors of the T_m predictions as a function of G•C base-pair content, number of base pairs, and magnesium concentrations. Similar accuracy is seen for various duplexes and magnesium concentrations. No systematic trends are observed. From 680 melting temperatures in the experimental data set, 96% are predicted within 1.3 °C and 99% are predicted within 2.0 °C. The average error of the T_m predictions is 0.5 °C.

Several additional terms and modifications of eq 16 were considered. Because they did not improve the fit, they are not included in the final equation. For example, if the term $1/[2(N_{bp} - 1)]^2$ was used in eq 16 instead of the $1/[2(N_{bp} - 1)]$ term, the goodness-of-fit decreased. Furthermore, addition of a $(\ln [Mg^{2+}])^2$ term to the I_{Nbp} relationship (eq 14) provided only marginal improvement of the fit, which was not statistically significant. This is consistent with Figure 6D, which shows that the dependence of I_{Nbp} on $\ln [Mg^{2+}]$ is approximately linear.

Table 3: Accuracy of Various T_m Magnesium Corrections Evaluated for Data Set of 92 DNA Duplex Oligomers in Magnesium Buffers When Effects of Monovalent Ions Are Negligible and Effects of Magnesium Ions Dominate

eq no.	T_m magnesium correction	χ_r^2	$\langle \lvert \Delta T_m \rvert \rangle_{AV}$ (°C)
16	this work	4.6	0.5
6	Peyret−SantaLucia	163.1	2.9
7	Ahsen−Wittwer−Schütz	185.3	3.0
9	Tan−Chen	176.4	3.3
8	Mitsuhashi	350.7	4.7

Since the Y_{GC} intercepts seem to approach a limiting value with increasing N_{bp} (Figure 5), we examined a model where oligonucleotide-length-dependent terms of eq 16 (*e*, *f*, *g* parameters) were neglected for longer duplexes ($N_{bp} \geq 20$). The remaining parameters were optimized and fitted to the experimental T_m data set. Predictions of melting temperatures for DNA oligomers from 20 to 60 base pairs were compared with the experimental data. This simplified correction function was found to be as accurate as eq 16 at low magnesium concentrations (~1.5 mM), but predictions in higher magnesium concentrations were less accurate. We conclude that the magnesium correction function depends significantly on oligonucleotide lengths even for these longer duplexes.

Accuracy and Limitations of the New T_m Magnesium Correction. Accuracy of the new eq 16 was compared with previous T_m magnesium correction equations using the experimental data sets from Tables 1 and S1. The average errors of these T_m predictions are summarized in Table 3. Predictions obtained using all of the earlier equations were less accurate, showing an average T_m error of 2.9 °C or larger, compared with an error of only 0.5 °C when the new eq 16 was used. These accuracy differences are statistically significant. Probabilities, *P*, that differences in χ_r^2 between eq 16 and the other corrections can occur by random chance are less than 10^{-300}. For certain sequences, the error in prediction of T_m using the previously published formulas (eqs 6−9) is quite large (10−18 °C). The largest error observed with eq 16 was 2.9 °C for the entire experimental data set of 680 measurements.

It is important to consider limitations of the new T_m magnesium correction function. Equation 16 was derived from melting data in the range of 0.5 mM to 600 mM Mg^{2+} at neutral pH (7−8) and is accurate in these ranges. The parameters were obtained under conditions in which the effects of monovalent ions were negligible. At higher concentrations, monovalent ions can significantly compete with magnesium ions. In this setting, the relationship between ion concentrations and T_m becomes more complex and some of the parameters require adjustment (see below).

It is the *free* magnesium concentration which affects duplex stability and enters into salt correction formula 16. In our experiments, magnesium ions were present in vast excess compared to DNA. Under these conditions, the free magnesium concentration is equal to the total magnesium concentration. When concentrations of Mg^{2+} and DNA phosphate groups are of the same magnitude, binding of magnesium ions to DNA must be taken into account. Such

Table 4: Experimental Melting Temperatures (°C) for 12 Duplex Oligodeoxynucleotides ($C_t = 2\ \mu M$) in Buffers of Various Magnesium and Monovalent Ion (K^+, $Tris^+$) Concentrations

	$[Mg^{2+}]$							
$[Mon^+]$	0 mM	0.5 mM	1.5 mM	3.0 mM	10 mM	20 mM	50 mM	125 mM
				TTCTACCTATGTGAT (ODN1)[a]				
1 mM		43.3	46.1	47.8	50.2	50.4		
5 mM		42.1	45.6	47.6	49.5	50.4	51.0	51.5
55 mM	39.3	42.5	44.7	46.2	49.1	49.6	51.0	51.5
105 mM	43.8	44.8	45.8	47.1	49.1	50.1	51.1	51.6
205 mM	47.7		48.1		49.9		51.1	51.4
605 mM	52.1		51.9		51.9		51.8	51.7
1.005 M	53.2		53.0		53.0		52.0	51.4
				GCAGTGGATGTGAGA (ODN2)[a]				
1 mM		52.3	55.1	56.5	58.1	58.7		
5 mM		51.9	54.7	56.2	58.2	58.8	59.2	59.0
55 mM	49.5	52.5	54.6	56.0	58.0	58.8	59.3	59.1
105 mM	53.8	54.6	55.8	56.6	58.2	58.9	59.4	59.4
205 mM	57.3		57.9		59.1		59.4	59.5
605 mM	61.6		61.3		61.1		60.2	59.5
1.005 M	62.4		62.3		61.7		60.3	59.6
				CAGCCTCGTCGCAGC (ODN3)[a]				
1 mM		61.9	64.1	65.3	66.8	67.3		
5 mM		61.1	64.2	65.1	67.2	67.5	67.5	67.3
55 mM	58.9	62.0	64.0	65.2	66.6	67.4	68.1	67.4
105 mM	63.1	63.8	65.0	65.7	67.5	67.5	67.8	67.2
205 mM	66.5		67.0		68.1		67.6	67.3
605 mM	69.9		69.8		69.4		67.9	67.3
1.005 M	70.6		70.3		70.1		68.1	66.9
				TGATTCTACCTATGTGATTT (ODN4)[a]				
1 mM		51.8	54.6	55.8	57.7	58.2		
5 mM		51.0	54.5	55.8	58.1	58.5	59.3	59.5
55 mM	47.6	51.1	53.8	55.4	57.9	58.9	59.4	59.5
105 mM	51.9	53.0	54.7	55.4	57.9	58.4	59.5	59.7
205 mM	56.1		57.0		58.7		59.4	59.9
605 mM	61.6		61.7		61.6		60.7	60.3
1.005 M	63.2		63.2		63.0		61.4	60.7
				AGCTGCAGTGGATGTGAGAA (ODN5)[a]				
1 mM		61.1	63.7	64.8	66.3	66.8		
5 mM		60.7	63.9	65.1	66.9	67.3	67.7	67.3
55 mM	57.8	61.1	63.2	64.6	65.8	67.1	67.8	67.5
105 mM	62.4	63.3	64.8	65.2	67.0	67.4	67.7	67.7
205 mM	66.4		67.1		68.1		67.5	67.8
605 mM	71.2		71.1		70.7		68.7	68.2
1.005 M	72.3		72.2		71.7		69.7	68.5
				CAGCCTCGTTCGCACAGCCC (ODN6)[a]				
1 mM		68.9	71.3	72.3	73.4	73.9		
5 mM		68.7	71.3	72.3	73.8	74.0	74.2	73.9
55 mM	65.0	68.7	70.8	71.9	73.2	74.0	74.2	73.8
105 mM	69.4	70.8	72.0	72.6	74.0	74.2	74.4	73.8
205 mM	73.5		74.0		74.8		74.4	73.9
605 mM	77.6		77.6		77.0		75.2	74.2
1.005 M	78.4		78.2		77.5		75.5	74.3
				GTTCTATACTCTTGAAGTTGATTAC (ODN7)[a]				
1 mM		57.2	59.7	60.8	62.4	63.0		
5 mM		56.3	59.4	60.7	62.6	63.1	63.8	64.0
55 mM	50.7	54.6	57.5	59.1	61.5	63.0	63.8	64.2
105 mM	55.9	57.3	58.9	60.0	62.2	63.2	63.9	64.3
205 mM	60.3		61.3		63.1		63.9	64.4
605 mM	66.1		66.2		66.0		65.2	64.9
1.005 M	68.0		67.9		67.5		66.1	65.5
				CTGGTCTGGATCTGAGAACTTCAGG (ODN8)[a]				
1 mM		65.6	67.7	68.7	69.8	70.3		
5 mM		65.1	67.6	68.5	70.1	70.3	70.7	70.6
55 mM	60.3	64.5	66.9	68.1	69.7	70.4	70.7	70.8
105 mM	64.9	66.2	68.0	68.8	70.3	70.7	71.0	70.9
205 mM	69.1		70.0		71.2		71.1	71.0
605 mM	74.2		74.1		74.0		72.5	71.6
1.005 M	75.8		75.6		75.2		73.2	72.3

Table 4: Continued

	[Mg^{2+}]							
[Mon^{+}]	0 mM	0.5 mM	1.5 mM	3.0 mM	10 mM	20 mM	50 mM	125 mM
				CAGTGGGCTCCTGGGCGTGCTGGTC (ODN9)[a]				
1 mM		73.5	75.3	76.2	77.3	77.6		
5 mM		73.3	75.9	76.6	78.0	78.0	78.2	77.4
55 mM	70.6	73.9	75.6	76.5	77.3	78.1	78.3	78.0
105 mM	74.3	75.6	77.2	77.4	78.7	78.4	78.3	77.8
205 mM	78.2		79.3		79.5		78.2	77.8
605 mM	82.6		82.6		81.9		79.4	78.3
1.005 M	83.4		83.3		82.6		79.8	78.4
				CTTAAGATATGAGAACTTCAACTAATGTGT (ODN10)[a]				
1 mM		61.0	63.1	64.1	65.5	66.0		
5 mM		60.5	63.2	64.4	65.9	66.4	67.1	67.1
55 mM	55.2	59.2	61.8	63.4	65.2	66.1	67.3	67.2
105 mM	60.2	61.5	63.0	64.0	66.0	66.6	67.2	67.2
205 mM	64.6		65.3		66.8		67.0	67.3
605 mM	70.4		70.4		70.1		68.5	68.1
1.005 M	72.4		72.0		71.4		69.6	68.5
				AGTCTGGTCTGGATCTGAGAACTTCAGGCT (ODN11)[a]				
1 mM		69.8	71.6	72.5	73.6	73.9		
5 mM		68.8	71.6	72.3	73.8	73.9	74.2	74.4
55 mM	64.6	68.5	71.0	72.1	73.8	74.1	74.4	74.7
105 mM	68.9	70.3	72.1	73.0	74.2	74.3	74.9	74.7
205 mM	73.2		74.3		75.1		74.7	74.9
605 mM	78.4		78.2		78.1		76.4	75.6
1.005 M	80.1		79.9		79.4		77.2	76.2
				GACCTGACGTGGACCGCTCCTGGGCGTGGT (ODN12)[a]				
1 mM		76.1	77.8	78.6	79.4	79.7		
5 mM		75.9	78.1	79.0	79.8	79.9	80.0	79.8
55 mM	73.2	76.5	78.0	79.0	79.5	80.0	80.3	79.6
105 mM	77.4	78.6	79.7	79.9	80.7	80.6	80.4	79.7
205 mM	81.2		81.8		81.8		80.5	79.9
605 mM	85.6		85.5		84.4		81.9	80.6
1.005 M	86.7		86.3		85.2		82.5	81.0

[a] DNA sequence (5′ to 3′) (duplex ID).

low magnesium concentrations occur rarely in biological applications.

The experimental data set employed to develop eq 16 contained DNA duplexes from 10 to 30 base pairs in length. An analysis of 40 and 60 base pair duplexes shows that eq 16 remains accurate in scaling T_m for these longer DNAs (see Table S2 of Supporting Information). Although these longer duplexes showed a single transition and had a well established T_m, they may melt in a non-two-state fashion. That is, in the narrow temperature range over which melting occurs (2−3 °C), partially melted duplexes may exist. However, the derivation of eq 16 was not dependent on the two-state assumption. It is valid for short oligomers (10−20 base pairs) which do melt in a two-state fashion as well as longer sequences that exhibit a single transition.

Although UV melting experiments reported in Tables 1 and S1 were conducted at a total single strand concentration of 2 μM, the utility of eq 16 is not limited to this DNA concentration. Melting studies were performed for a subset of 21 sequences in 1.5 mM Mg^{2+} buffer using differential scanning calorimetry where DNA concentrations were 90-fold higher ($C_t = 180$ μM). See Table S4 of the Supporting Information. The T_m values under these conditions were predicted using eq 16 while the melting temperatures obtained from earlier calorimetric experiments in 1 M Na^+ (*33*) were used as the reference point. Melting temperatures of the DSC data set were predicted with an accuracy ($\langle|\Delta T_m|\rangle_{AV} = 0.4$ °C) similar to the accuracy of the UV melting data set ($\langle|\Delta T_m|\rangle_{AV} = 0.5$ °C).

Deoxynucleoside Triphosphates Decrease Effects of Magnesium Ions. PCR reactions require deoxynucleoside triphosphates (dNTPs) in mixture with short oligomer primers, probes and longer nucleic acid targets. Magnesium ions bind to all of these components, and this binding decreases the concentration of free magnesium ions. As DNA synthesis proceeds during PCR, dNTPs are incorporated into the products and pyrophosphate is released. Pyrophosphate also binds magnesium ions. Complex linked equilibria of Mg^{2+} binding occur. It was empirically observed in PCR reactions that magnesium ion concentration must exceed the total concentration of dNTPs to achieve efficient amplification (*3, 26*). It has been suggested that the free magnesium ion concentration, [Mg^{2+}], is a critical parameter to be optimized in PCR and that it can be estimated from the difference between the total magnesium ion and the total dNTP concentrations (*15*). To verify this notion, melting experiments of DNA duplexes were done in the presence and absence of dNTPs. Because DNA and dNTP molecules absorb light at similar wavelengths, ultraviolet spectroscopy is not a suitable technique to study denaturation of DNA duplexes when dNTPs are present in excess. We therefore employed differential scanning calorimetry (DSC). Until recently, DSC experiments required the use of high DNA concentrations (~100 μM), which are more than 2 orders of magnitude larger than the concentrations of primers typically used in PCR experiments

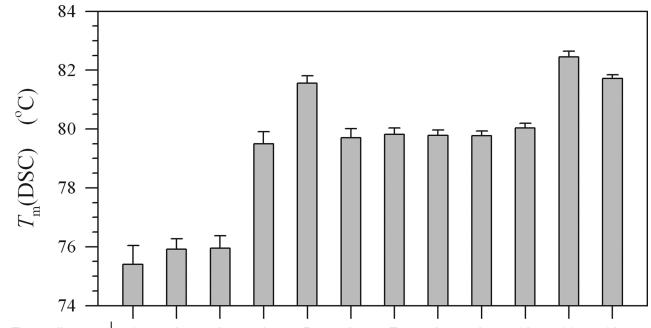

Exper. #	1	2	3	4	5	6	7	8	9	10	11	12
Free [Mg^{2+}]	0.0	0.0	0.0	0.5	1.5	0.5	0.5	0.5	0.5	0.5	3.0	1.5
c(Mg^{2+}) (mM)	0.0	0.0	0.0	0.5	1.5	1.5	1.5	1.5	1.5	1.5	3.0	3.0
c(dNTP) (mM)	0.0	1.0	1.0	0.0	0.0	1.0	1.0	1.0	1.0	1.0	0.0	1.5
		dATP	mix			dATP	dGTP	dCTP	dTTP	mix		dATP

FIGURE 7: Experimental melting temperatures of the 60-mer duplex (see Materials and Methods) were obtained using DSC at low DNA concentration ($C_t = 2\ \mu M$). Buffers contained 50 mM KCl, 10 mM Tris-HCl (pH = 8.3) and various amounts of magnesium ions and deoxynucleotide triphosphates. Concentrations (mM) used in each experiment are indicated below the graph. The first row is the free [Mg^{2+}], which is calculated as the difference between total Mg^{2+} and dNTP concentrations. dNTP "mix" contained equimolar concentrations of dATP, dGTP, dCTP and dTTP. The sum of their concentrations is shown in the table below the graph.

(<1 μM). However, new ultrasensitive calorimeters are available that allow measurement of T_m values using less than 5 μM concentration of a duplex (*48*). We studied a sixty base pair long DNA duplex (see Materials and Methods) that exhibited a single, sharp reproducible melting transition. Melting temperatures were determined at the same DNA concentration ($C_t = 2\ \mu M$, i.e., 0.06 mM/base pair) while buffer composition was varied. Results are presented in Figure 7. Experiments 1−3 were done in 50 mM KCl and 10 mM Tris-HCl. We found that addition of dATP or an equimolar mixture of all four dNTPs did not affect the T_m when magnesium was absent. Experiments 4−12 contained various amounts of Mg^{2+} ions. Comparison of experiments 4, 5, and 11 shows that raising the magnesium concentrations from 0.5 to 3 mM increased the T_m. Addition of 1 mM dATP to the 1.5 mM Mg^{2+} buffer decreased the T_m of the duplex from 81.6 ± 0.3 (experiment 5) to 79.7 ± 0.3 °C (experiment 6), which is identical within experimental error to the melting temperature of that duplex in 0.5 mM Mg^{2+} buffer alone (experiment 4, 79.5 ± 0.4 °C). Analogous observations were made for stability of the duplex in 3.0 mM Mg^{2+} plus 1.5 mM dATP (experiment 12). The duplex had a T_m of 81.7 ± 0.1 °C, which is equal to its T_m in 1.5 mM Mg^{2+} buffer when no dATP was present (81.6 ± 0.3 °C, experiment 5). Experiments 6−10 in Figure 7 demonstrate that addition of dATP, dGTP, dTTP, and dCTP impact T_m by similar amounts. Affinity for magnesium ions is grossly similar between different dNTPs and is primarily determined by properties of the triphosphate and ribose groups (*49, 50*).

These results confirm that dNTPs bind magnesium ions stochiometrically (1:1) with high affinity and that the remaining free magnesium ions determine the melting temperature of a DNA duplex. Therefore, in connection with the use of T_m correction eq 16, the magnesium ion concentration should be adjusted for the total concentration of dNTPs. That is, the free concentration of magnesium ions, [Mg^{2+}], can be assumed to equal the difference between the total magnesium concentration, c_{Mg}, and the total concentration of dNTPs, c_{dNTP}. This relationship will not hold if the total dNTP concentration is larger or similar (within 20%) to the total magnesium ion concentration. In that case, the free magnesium ion concentration will be very low and may be approximated from the relationship for the Mg-dNTP association constant,

$$K_a = \frac{c_{Mg} - [Mg^{2+}]}{[Mg^{2+}](c_{dNTP} - c_{Mg} + [Mg^{2+}])} \qquad (17)$$

By using published experimental data for ribonucleotides (*49*−*51*), we estimate that K_a is approximately 3×10^4 for the Mg−dNTP complex in a PCR buffer of 50 mM KCl and 10 mM Tris. In situations when the free magnesium ion concentration is very low, effects of monovalent ions on duplex stability will often be dominant.

Competition between Magnesium and Monovalent Ions in Duplex Stabilization. Equation 16 and its parameters were determined in solutions with very low concentrations of Tris cations (1−5 mM) where magnesium ions are dominant in their effects on melting temperatures. We next examined duplex stability in mixed buffers containing significant amounts of both magnesium and monovalent ions. Figure 8A illustrates that the observed T_m effects are a complex function of monovalent ion and magnesium ion concentrations. The highest T_m was achieved in 1 M KCl solution; the maximal T_m reached in magnesium solutions was lower. This might not be true for very short oligomers ($N_{bp} \leq 10$) where Mg^{2+} ions may provide larger stabilizing effects than a 1 M solution of monovalent ions (*13, 52*).

Cations bound to DNA are subject to an ion-exchange reaction in which the associated cations are released into bulk solvent. NMR line-shape analysis (*53*), UV melting (*5, 14*), electrophoresis (*54, 67*) and buffer equilibration−atomic emission spectroscopy (*68*) experiments have demonstrated that the extent of Mg^{2+} binding to DNA decreases with increasing monovalent ion concentration indicating that magnesium and monovalent ions compete for DNA binding. Table 4 presents results of melting experiments for 12 DNA duplexes 15 to 30 base pairs long. Their GC content ranged from 30 to 73%. For each buffer and oligonucleotide, the T_m value in the mixed buffer was compared to T_m values in reference buffers, which were missing either potassium ions (first rows of T_m data in Table 4) or magnesium ions (first column of T_m data). Depending on buffer composition, either monovalent or magnesium ions were found to be dominant and largely determine the melting temperature, the remaining ions having only minor effects on duplex stability ($\Delta T_m < 3$ °C). At each Mg^{2+} concentration, a concentration of monovalent ions is eventually reached at which the T_m is accurately predicted by the effect of monovalent ions alone (eq 4). This analysis determined the crossover point at which the dominant ion changes from magnesium to monovalent ions. This did not occur at a unique value of the ratio [Mg^{2+}]/[Mon^+]. With increasing monovalent ion concentration, this ratio was found to increase. However, the ratio $R = ([Mg^{2+}])^{1/2}/[Mon^+]$ at this point is independent of ion concentrations and nearly identical for all 12 sequences. The value of R at the crossover point is 0.22 $M^{-1/2}$. This provides a convenient measure to determine whether divalent or monovalent ions are dominant in their effects on T_m (Figure 8B). If R is equal to or greater than 0.22, magnesium effects dominate and T_m correction eq 16 should be employed (the influence of monovalent ions can be neglected). If R is less

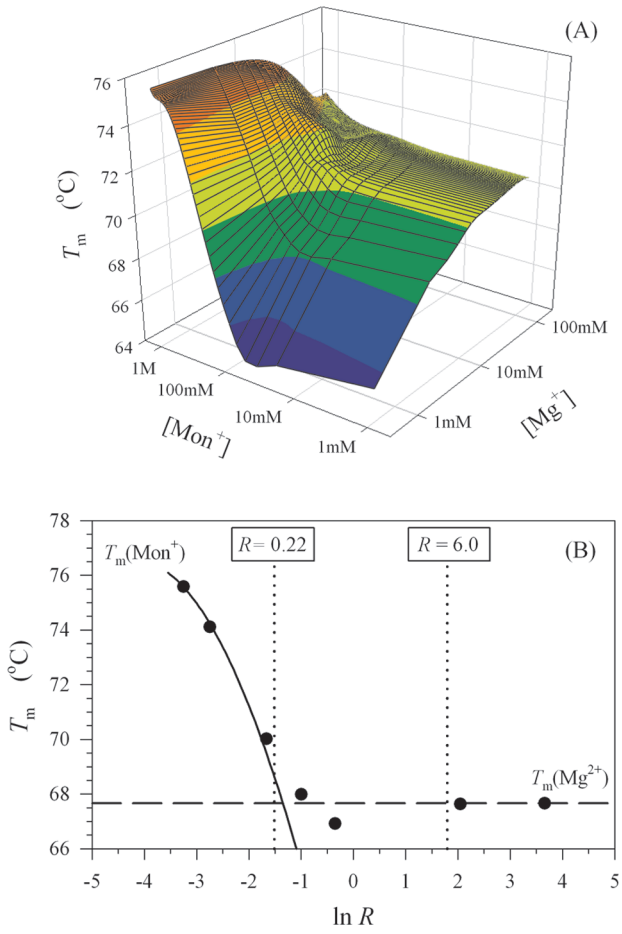

FIGURE 8: Competitive effects of K^+ and Mg^{2+} examined for the 25 bp long duplex, ODN8, CTGGTCTGGATCTGAGAACTTCAGG. (A) Dependence of T_m on concentrations of magnesium and monovalent ions. (B) Solid circles are T_ms plotted against ln R, where $R = [Mg^{2+}]^{0.5}/[Mon^+]$. Buffers are composed of constant 1.5 mM Mg^{2+} while KCl concentration varies. The solid line shows melting temperatures predicted by sodium salt correction (eq 4) when no Mg^{2+} is present. The dashed line indicates T_m in magnesium buffer when no KCl is present. The dominant ion crossover that occurs on average at R of 0.22 is indicated with the dotted vertical line.

than 0.22, the T_m correction for monovalent ions (eq 4) should be used (*33*). Under these conditions, monovalent ions are dominant and determine T_m, and the presence of Mg^{2+} can be ignored.

Figure 8B also illustrates that the addition of K^+ at concentrations of 50−100 mM to magnesium buffers can paradoxically decrease the value of T_m by 1−2 °C. This effect, although small, was observed for all 12 sequences. It occurs for values of R in the range of 0.22 to 6.0 and is most pronounced for oligonucleotides of low GC content. A similar effect was observed for genomic DNAs (*5, 17*). Importantly, PCR buffers fall in this range of R values. Therefore, it seemed worthwhile to determine if the T_m prediction could be improved by taking this effect of ion competition into account. This is best achieved by allowing the parameters a, b, c, d, e, f, g of eq 16 to vary with monovalent ion concentrations. When we allowed only two parameters to vary with $[Mon^+]$ and kept the remaining parameters constant, no significant improvements in the accuracy of T_m predictions were seen. When sets of three parameters were allowed to change, the best improvements of T_m predictions were observed for the set where parameters a, d, and g varied. Potential empirical equations for parameters were tabulated using the TableCurve 2D software package (SYSTAT Software Inc., Richmond, CA). The following simplest equations were selected:

$$a = 3.92 \times 10^{-5}\left(0.843 - 0.352\sqrt{[Mon^+]} \times \ln[Mon^+]\right) \quad (18)$$

$$d = 1.42 \times 10^{-5}[1.279 - 4.03 \times 10^{-3} \ln[Mon^+] - 8.03 \times 10^{-3}(\ln[Mon^+])^2] \quad (19)$$

$$g = 8.31 \times 10^{-5}\,[0.486 - 0.258 \ln[Mon^+] + 5.25 \times 10^{-3}(\ln[Mon^+])^3] \quad (20)$$

Concentrations are in units of mol/L. Use of eq 16 modified with parameters a, d, g adjusted according to eqs 18−20 predicts the drop in T_m observed when R lies in the range from 0.22 to 6.0. The overall fit of the data in Table 4 is also improved slightly when parameters a, d, g of eq 16 are allowed to vary (Table 5).

A general scheme for selecting the most accurate T_m correction function to employ based upon the relative amounts of monovalent and magnesium cations is shown in Figure 9. Starting from experimentally measured reference T_ms in 1.0 M Na^+ buffer (*33*), melting temperatures from Table 4 were predicted according to this algorithm as well as previously published equations. Statistical comparisons between these methods are reported in Table 5. The most accurate predictions, with an average error of 0.8 °C, are obtained when parameters a, d, g are allowed to vary with monovalent ion concentration. If the parameters of eq 16 are set to constant values from Table 2, the accuracy is decreased ($P < 2 \times 10^{-5}$). Previously published eqs 6−9 are significantly less accurate ($P < 10^{-118}$).

Equations 6, 7, 8, 9 and the algorithm from Figure 9 were used to predict melting temperatures for a validation data set of duplex DNA oligomers in Table S2 of the Supporting Information. This independent validation data set includes both published T_m values from other groups and new data presented here, comprising 69 unique pairs of T_m measurements for 39 sequences ranging in length from 9 to 60 base pairs. These sequences were not used to develop our new T_m magnesium salt correction formulas, so this is a more meaningful test of performance than can be achieved using the original derivation data sets (Tables 1, S1 and 4). Experimentally measured melting temperatures in the absence of magnesium ions (buffer 1) were used as the reference T_m, and various correction formulas were applied to predict T_m values in the presence of magnesium ions (buffer 2). Statistical comparisons of the results are shown in the last two columns of Table 5. The new magnesium correction algorithm predicted melting temperatures with the lowest error (0.9 °C) and χ_r^2 value. The predictions obtained from eqs 6−9 were significantly worse ($P < 9 \times 10^{-5}$). The algorithm shown in Figure 9 is therefore currently the most accurate method to scale melting temperatures between solutions of different monovalent and magnesium cation concentrations.

Example of Calculations Using the New T_m Magnesium Correction. Below we illustrate use of algorithm in Figure 9 to estimate the melting temperature for a 20 base-pair duplex, 5′-AAGGCGAGTCAGGCTCAGTG-3′ with 12 G·C base pairs ($f_{GC} = 12/20 = 0.600$), in 1.5 mM Mg^{2+}, 10 mM Tris-HCl buffer. A reference T_m(1 M Na^+) of 76.3 °C was measured (*33*) in 1 M Na^+ and $C_t = 2$ μM. Since total

Table 5: Accuracy of Various T_m Magnesium Correction Equations Evaluated in Buffers Where Magnesium and Potassium Ions Compete in Their Effects on DNA Duplex Stability

		data from Table 4[a] (n = 456)		validation data set[b] (n = 69)	
eq no.	T_m correction function	$\langle\lvert\Delta T_m\rvert\rangle_{AV}$ (°C)	χ_r^2	$\langle\lvert\Delta T_m\rvert\rangle_{AV}$ (°C)	χ_r^2
4, 16, 18−20	this work allowing parameters a, d, g to vary with [Mon$^+$]	0.8	10.0	0.9	22.8
4, 16	this work with constant parameters	0.9	15.3	1.0	23.2
6	Peyret−SantaLucia	2.6	137.5	1.6	66.1
7	Ahsen−Wittwer−Schütz	2.9	163.1	1.9	81.0
9	Tan−Chen	2.6	116.5	1.9	105.1
8	Mitsuhashi	3.8	250.0	2.4	102.8

[a] Buffers where both Mg^{2+} and K^+ were present. [b] Data from Table S2 of the Supporting Information.

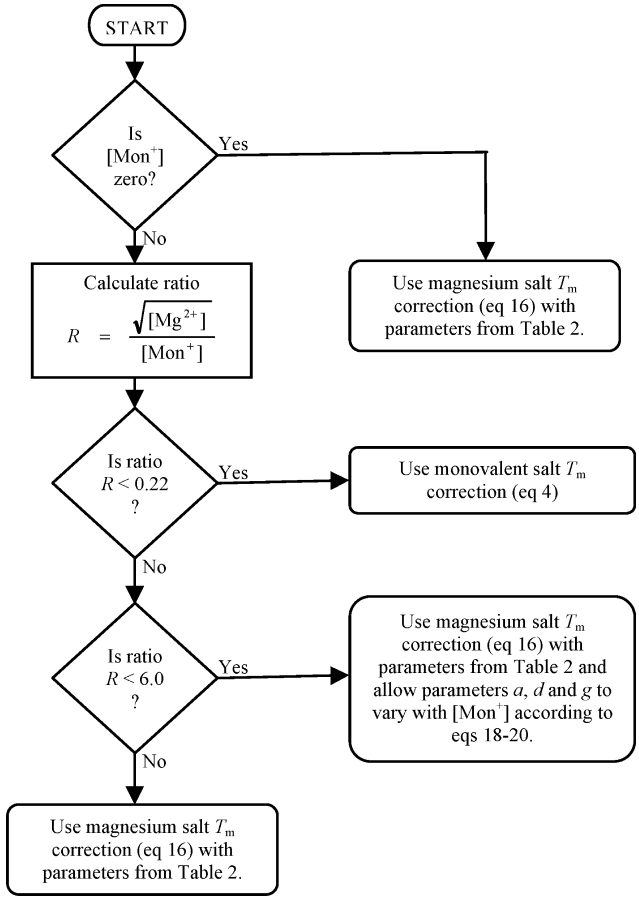

FIGURE 9: Flowchart for algorithm used to select the most accurate T_m salt correction equation depending on the relative amounts of monovalent and magnesium cations present.

monovalent ion concentration is 5 mM, $R = (0.0015)^{1/2}/0.005 = 7.75$. As the ratio R is larger than 0.22, magnesium ions will exhibit dominant effects on T_m. Because R is larger than 6.0, parameters a, d, g in the magnesium T_m correction eq 16 do not need to vary with [Mon$^+$] but can be taken directly from Table 2,

$$\frac{1}{T_m(Mg^{2+})} = \frac{1}{T_m(1\ M\ Na^+)} + 3.92\times10^{-5} - 9.11\times10^{-6}\ln 0.0015 + 0.6(6.26\times10^{-5} + 1.42\times10^{-5}\ln 0.0015) + \frac{1}{2(20-1)}[-4.82\times10^{-4} + 5.25\times10^{-4}\ln 0.0015 + 8.31\times10^{-5}(\ln 0.0015)^2] = \frac{1}{(76.3+273.15)} + 7.0537\times10^{-5} = 2.9322\times10^{-3}\ K^{-1}$$

The predicted $T_m(Mg^{2+})$ under these conditions is 341.0 K (67.9 °C). This compares to a value of 68.5 °C measured experimentally

DISCUSSION

Melting temperatures of DNA duplex oligomers were studied systematically in buffers containing Mg^{2+}, K^+ and $Tris^+$ ions. Novel T_m magnesium correction functions were developed that can be used to accurately scale melting temperatures between various salt environments. Statistical analysis showed that use of these new formulas significantly improves T_m predictions. Previous T_m magnesium correction eqs 6−8 assume "equivalent" effects of sodium and magnesium ions on duplex stability. Our analysis indicates that the effects of divalent cations on T_m differ both quantitatively and qualitatively from the effects of monovalent cations. The dependence of T_m on GC content is different for Mg^{2+} and monovalent ions. The relationship to oligonucleotide length is also different. Duplex melting demonstrates end-effects in magnesium solutions, which led to inclusion of terms dependent on oligonucleotide length into eq 16. In contrast, length dependent terms are unnecessary for the T_m correction function for sodium ions (eq 4) (*33*). T_m changes mediated by monovalent ions are independent of the number of base pairs and depend primarily on the f_{GC}. The concept of "equivalency" of Na^+ and Mg^{2+} effects is therefore not justified. As a result, algorithms based on insertion of an "equivalent" sodium ion concentration into equations developed to predict the effect of monovalent ions on T_m fail to give accurate estimates of T_m in magnesium solutions.

The TBI theory developed by Tan and Chen (*7, 46*) represents an improvement from earlier theoretical models in that it does predict the saturation effect of magnesium ions on T_m (see Figure 3). However, the overall accuracy of the prediction of T_m with this model is not improved (Table 3). It may be possible to modify certain assumptions made in the TBI theory to more accurately predict experimental melting data. However, even with such improvements it would not appear possible to account for the observed sequence dependent effects using electrostatic principles alone.

The saturation effect on T_m seen with magnesium occurs at lower concentrations the higher the GC content of the duplex (Figure S3). A similar effect was observed previously for the binding of Na^+ ions (*33*). This sequence specific behavior is consistent with a study of repeating polymers using ^{25}Mg NMR spectroscopy (*55*), in which G·C base pairs were found to bind Mg^{2+} up to 100-fold more strongly than A·T base pairs. Sequence dependent Mg^{2+} binding was also

detected when hydration of DNA duplexes was investigated using ultrasonic velocity measurements (*56*). DNA A·T base pairs were proposed to interact with magnesium ions by outer-sphere complex formation, while G·C base pairs exhibited substantial dehydration changes typical for inner-sphere complexes.

Two modes of ion binding have been suggested for the interaction of metal ions with DNA (*23, 56*). "Site binding" refers to specific binding of the ion to negatively charged groups or pockets on nucleic acids. This more intimate interaction is often observed in tertiary folds of RNA molecules where phosphates are clustered (*23*). Unique, specific sites take up an integral number of ions. Site-bound ions may lose some of their coordinated water molecules. The second binding mode, "diffuse binding", refers to all nonspecific interactions of ions with DNA where ions are highly delocalized in areas surrounding the DNA molecule. Specifically, this refers to the process whereby magnesium or monovalent cations form an ionic sleeve around single-stranded or double-stranded DNA and neutralize its negatively charged phosphate backbone. Localization of diffusely bound ions is difficult to determine experimentally as the ions are relatively free to move within areas of similar electrostatic potential.

Diffuse magnesium ions are thought to be bound through "outer-sphere" complexes where magnesium ions coordinate six water molecules, $[Mg(H_2O)_6]^{2+}$, and the water molecules establish a network of hydrogen bonds. This was observed using ^{25}Mg NMR (*57*) and crystallographic studies (*58, 59*). Electrostatic effects, therefore, cannot be completely decoupled from changes of hydration caused by counterion binding (*56*). Changes in the solvation shells of participating ions and hydrogen binding between water molecules in the hydration shells of Mg^{2+} and Na^+ may make important contributions to the energetics of cation binding to DNA.

In our experiments, we found a small but significant decrease in T_m at very high magnesium concentrations (Figure 4). This agrees with a previous study of the duplex dGCATGC (*13*) and melting experiments of genomic DNAs (*18, 19, 60*). These destabilizing effects may be caused by binding of magnesium to additional sites on denatured DNA (e.g., bases), by conformational changes of DNA and/or by ion−ion repulsions in the ionic atmosphere surrounding the DNA duplex (*7*). Magnesium ions have a strong preference for association with phosphate groups (*1, 49*). If binding of magnesium ions to the bases does occur, the association constants must be several orders of magnitude smaller than the binding constants of magnesium ions with the phosphate backbone.

Binding of Magnesium Cations to Single Stranded versus Double Stranded DNA. Magnesium ions bind to nucleic acids in both the duplex and single strand states but to a greater degree in the duplex form. Denaturation of a duplex is therefore accompanied by a net release of Δn magnesium ions. Assuming a two-state melting transition, the value of Δn can be estimated from the dependence of the melting temperature on magnesium ion concentration (*5*):

$$\Delta n = \frac{d\left(\frac{1}{T_m}\right)}{d \ln[Mg^{2+}]} \frac{\Delta H^\circ}{R} \qquad (21)$$

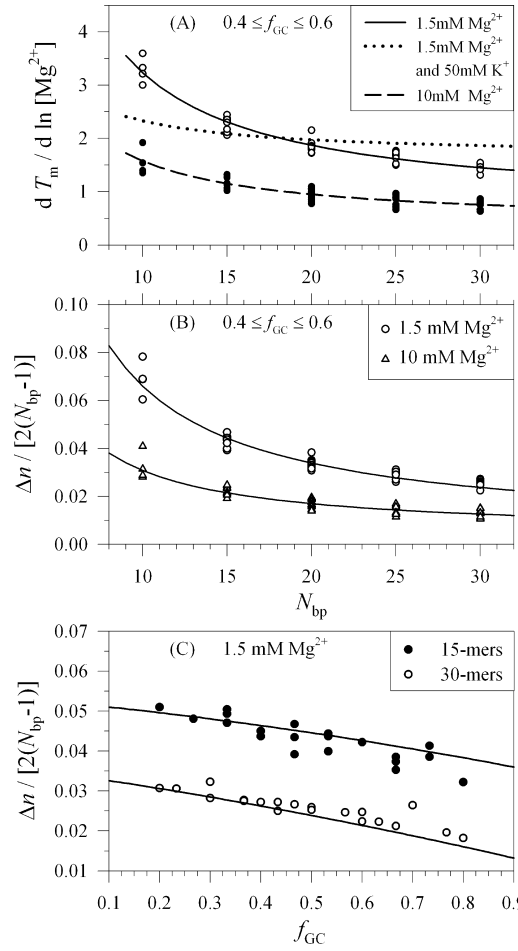

FIGURE 10: Release of magnesium ions associated with duplex denaturation. (A) Experimental values of $dT_m/d(\ln [Mg^{2+}])$ are shown in 1.5 mM (open circles), and 10 mM (closed circles) magnesium buffers as well as in the buffer containing both 1.5 mM $MgCl_2$ and 50 mM KCl (dotted line). The GC content of oligonucleotides ranges from 40 to 60%. For the sake of clarity, experimental data for individual duplexes are not shown for the last buffer; the relationships are approximated with lines fitted to experimental data points. (B) The number of released magnesium ions per phosphate group is plotted as a function of oligonucleotide lengths. Solid lines were predicted from eqs 16 and 21, and from the published average dependence of ΔH° values on oligonucleotide length (*35*). (C) The number of released magnesium ions per phosphate group decreases with increasing GC content in 1.5 mM Mg^{2+} buffer. These relationships are predicted reasonably well using eqs 16 and 21 (solid lines).

Figure 10 shows analysis of Δn values normalized to the number of phosphate groups as a function of oligonucleotide length and f_{GC}. The values of $d(1/T_m)/d(\ln [Mg^{2+}])$ were calculated for each DNA duplex from quadratic fits to plots of $1/T_m$ versus $\ln [Mg^{2+}]$. The enthalpy of duplex denaturation, ΔH°, was calculated from the unified nearest-neighbor thermodynamic parameters (*31, 66*) and was assumed to be independent of magnesium ion and monovalent ion concentrations (*31, 33*). The ΔH° values were also measured directly using DSC for a set of 21 sequences in 1.5 mM Mg^{2+} buffer (Table S3, Supporting Information). The enthalpies were found to be similar in magnesium and sodium buffers. Experimental errors are in the range of 5−10%. Therefore, the assumption that the enthalpies of duplex denaturation are salt independent is valid under the conditions studied. Equation 21 was used to calculate Δn values for oligonucleotides from 10 to 30 base pairs. Shorter oligomers (10−15

base pairs) are likely to melt in a two-state manner. The duplexes longer than 15 base pairs may show deviations from the two-state melting behavior. However, eq 21 still holds for these longer duplexes because their shapes of melting profiles are not dependent on the counterion concentration. Analysis that proves this statement is complex and requires a considerable amount of material. It is therefore shown in the end of the Supporting Information.

Values of Δn include contributions from the diffusely bound as well as from the site-bound Mg^{2+} ions. Since the value of Δn is derived from purely thermodynamic considerations, it provides no explicit information about the location of ions near the DNA molecule. Nevertheless, Δn is a useful estimate of the overall changes in ion association when the duplex denatures. Figure 10 illustrates that both the$dT_m/d(\ln [Mg^{2+}])$ and the value of Δn decrease as the free Mg^{2+} concentration is increased from 1.5 to 10 mM. At higher concentrations, the stabilizing effect of magnesium on the duplex reaches a maximum (see Figure 4). These observations suggest that magnesium ion binding to the single strands increases and eventually saturates as the magnesium ion concentration of the buffer increases.

Both the value of $dT_m/d(\ln [Mg^{2+}])$ and the value of Δn per phosphate decrease with increasing oligonucleotide length (see panels (A) and (B) of Figure 10). This is a result of significant end effects in magnesium buffers. Association of cations with ends of both single stranded and double stranded oligonucleotides is lower than with their interior. Thus the number of bound ions per phosphate group is predicted to increase with N_{bp} as the interior domain becomes larger. However, a larger increase is expected for duplexes because of their higher charge density (*11, 46*). Since Δn per phosphate group measures the difference of ion association between the duplex and the complementary single strands, it is expected to increase with N_{bp}. This was observed experimentally for a set of $d(TA)_N$ hairpins (*63*) with Na^+ as the counterion. DNA duplexes formed from two complementary strands in Na^+ buffers do not show a significant dependence of Δn on N_{bp} (*33*). This may be due to the fact that the number of negative charges per molecule is halved upon strand separation and thereby masking the Coulombic end effects (*11, 61, 62*). Surprisingly, we observe the opposite end effects with magnesium ions (Figure 10). The value of Δn per phosphate *decreases* when oligonucleotide length is increased. Can polyelectrolyte models based on electrostatic interactions explain the different behavior of Na^+ and Mg^{2+} counterions? Additional theoretical studies will be needed to clarify the interpretation of these results.

Figure 10A also shows that the end effect observed in magnesium buffers is substantially diminished by the addition of monovalent ions (50 mM KCl). Although Mg^{2+} ions remain dominant in 1.5 mM Mg^{2+} and 50 mM K^+, the values of Δn per phosphate decrease much less with N_{bp} in this mixed buffer than in 1.5 mM Mg^{2+} buffer where no K^+ was present. This observation is consistent with the study of DNA duplex stability in solutions of sodium ions (*33*) where the Δn per phosphate was found to be independent of oligonucleotide length.

Figures 10B and 10C demonstrate that our new T_m magnesium correction (eq 16) provides reliable predictions of Δn values. The derivative of $d(1/T_m)/d(\ln [Mg^{2+}])$ was entered into eq 21 to obtain an estimate of Δn. The relationships between hybridization enthalpies of duplex annealing and N_{bp} as well as f_{GC} were approximated using the unified nearest-neighbor parameters (*31, 35, 66*) ($\Delta H^\circ = -8.23(N_{bp} - 1) + 2.4$ kcal/mol for duplexes containing 50% GC; $\Delta H^\circ = -100.5 - 25.9 f_{GC}$ kcal/mol for 15-mers and $\Delta H^\circ = -212.6 - 49.9 f_{GC}$ kcal/mol for 30-mers). Predicted Δn values shown by the solid lines in Figures 10B and 10C agree well with experimental observations.

Competitive Behavior of Monovalent and Magnesium Cations. Effects of ions on duplex stability are linked to the energetics of ion binding around the folded and the unfolded DNA molecules. These ion distributions are affected by bulk ionic concentrations. Sodium and magnesium ions act in concert to increase T_m at *low* magnesium/DNA concentration ratios (below 0.5 Mg^{2+} ions per nucleotide) (*5*). At higher magnesium/nucleotide ratios, magnesium and monovalent ions compete in their binding to DNA (*5, 12, 14*). We have found that the critical determinant whether magnesium ions or monovalent ions are dominant is the value of the ratio $R = ([Mg^{2+}])^{1/2}/[Mon^+]$. Figure 8B illustrates the nature of this competition for a 25 base pair long duplex. When the ratio R is greater than 6, magnesium ions are dominant and the ionic clouds surrounding both single and double stranded DNA contain mostly Mg^{2+} counterions. Under these conditions, the effects of monovalent ions on the T_m are negligible. Data from which eq 16 was derived (Tables 1 and S1) were from experiments where all R values were greater than 20. As the K^+ concentrations increase, the ratio R decreases. When the value of R falls below ~6, bound magnesium ions are being displaced by K^+. As a result, parameters of eq 16 change (eqs 18−20). The melting temperature decreases slightly when potassium ions are added to solutions of magnesium ions under these conditions. This was observed for all 12 duplexes studied (see Table 4). The slight destabilization is predicted by polyectrolyte theory (*5, 6, 9*) and has also been observed with genomic DNAs (*17*). Under these conditions, the bulk potassium concentration is much higher than the bulk magnesium concentration. Therefore, the diffuse Debye−Hückel ion atmosphere will be composed mostly of potassium ions. Because of magnesium counterion condensation, a larger effective charge is present on single strands than on double strands and single strands are therefore stabilized more by addition of monovalent ions due to Debye−Hückel screening.

When the value of R falls below 0.22, monovalent ions become dominant. At this point, replacement of the magnesium ions by potassium in the ionic clouds surrounding DNA is essentially complete. The dependence of the melting temperature on the counterion concentration thereafter follows the T_m correction function developed previously for monovalent ions alone (eq 4). Duplex stability then rises with increasing monovalent ion concentration. At 1.5 mM Mg^{2+}, the crossover point is at ~180 mM K^+. At higher concentrations of magnesium, the crossover point shifts to progressively higher concentrations of monovalent ions. Nakano et al. (*14*) studied Na^+−Mg^{2+} competition for the single duplex d(GCCAGTTAA). We calculated from their Figure 6 that the dominant ion changed from magnesium to sodium at value of R equal to 0.24 in good agreement with our findings.

The ionic atmosphere around DNA as a function of Mg^{2+} and Na^+ concentrations has been modeled using Monte Carlo simulations, Poisson−Boltzmann calculations (*12, 64*) and

the hypernetted chain integral method (*65*). Using the nonlinear Poisson−Boltzmann equation, Rouzina and Bloomfield (*64*) predicted that, to maintain the same proportion of sodium and magnesium ions bound to DNA while varying the bulk ionic composition, one should keep the ratio $[Mg^{2+}]/[Na^+]^2$ constant. A similar conclusion can be inferred from the theoretical study of Bacquet and Rossky (*65*). Our experimental results now provide convincing support for these predictions.

Effects of Magnesium Ions on Transition Enthalpies, Entropies and Free Energies. Useful salt-correction equations for free energies, $\Delta G°$, and entropies, $\Delta S°$, of DNA hybridization can be developed from eq 16 if the following assumptions are made: (i) Duplex melting is a two-state process. (ii) Counterion effects are mostly entropic (*31, 61, 66*). (iii) Enthalpies and entropies of DNA melting reactions are temperature independent, i.e., ΔC_p is zero. Although the last assumption may not be correct over a wide range of temperatures, it is reasonable within the narrow range of temperatures between $T_m(Mg^{2+})$ in a magnesium buffer and the reference $T_m(1\ M\ Na^+)$ in 1 M Na^+ buffer (see Table S3, Supporting Information). Using the relationship $1/T_m = \Delta S°/\Delta H° + (R/\Delta H°) \ln [C_t/4]$, eq 16 can be rearranged to obtain the following equations for transition entropies:

$$\Delta S°(Mg^{2+}) = \Delta S°(1\ M\ Na^+) + \Delta H°\left\{a + b\ln[Mg^{2+}] + f_{GC}(c + d\ln[Mg^{2+}]) + \frac{e + f\ln[Mg^{2+}] + g(\ln[Mg^{2+}])^2}{2(N_{bp} - 1)}\right\} \quad (22)$$

and transition free energies at 37 °C,

$$\Delta G°_{37}(Mg^{2+}) = \Delta G°_{37}(1\ M\ Na^+) - 310.15\Delta H°\left\{a + b\ln[Mg^{2+}] + f_{GC}(c + d\ln[Mg^{2+}]) + \frac{e + f\ln[Mg^{2+}] + g(\ln[Mg^{2+}])^2}{2(N_{bp} - 1)}\right\} \quad (23)$$

The units of $\Delta H°$ and $\Delta G°_{37}$ are cal/mol. These relationships should be useful for calculating energetics of DNA folding in the presence of magnesium ions.

Implications for PCR and DNA Sequencing. Accurate prediction of T_m in specific reaction conditions is a fundamental step when designing oligodeoxynucleotides for use in PCR, DNA sequencing and other molecular biology applications. T_m prediction is particularly important when working with closely related sequences (allelic variants, single nucleotide polymorphisms, etc.) or when designing multiplex reactions where a large number of primers must function together. We have studied a number of the solution components that can affect DNA duplex stability and therefore impact the design of DNA primers and probes.

Buffers used in molecular biology experiments generally contain a mixture of monovalent cations (Na^+ or K^+) and Mg^{2+}. As shown in Figure 2, the effects of sodium and potassium ions on duplex stability are equivalent. This is true even under conditions in which Na^+ and K^+ compete with Mg^{2+} for binding to DNA. Therefore, nearest-neighbor parameters and salt correction formulas developed for buffers containing Na^+ can be used interchangeably with K^+.

We have found that the effect of Mg^{2+} on T_m is dominant over monovalent cations under typical reaction conditions used for PCR and DNA sequencing ($[K^+] = 20-100$ mM and $[Mg^{2+}] = 1.5-5$ mM). Values of R range from about 0.3 to 4 $M^{-1/2}$. Accurate treatment of the effect of Mg^{2+} on T_m is, therefore, very important in the design of DNA primers and probes for these assays. Using the algorithm of Figure 9 with the correction formulas presented herein, the T_m can be predicted within an average accuracy of 1 °C. Earlier models are less accurate and in some cases lead to large errors (>10 °C). The procedure of converting the Mg^{2+} component to an "equivalent Na^+ concentration" is not justified. The influence of magnesium and monovalent cations on DNA duplex stability differ with respect to both f_{GC} and oligonucleotide length and must be treated differently.

Although metal ions present in reaction buffers (Na^+, K^+, Mg^{2+}) have the greatest impact on T_m, other components contribute and should be taken into account. Most buffers used in molecular biology applications rely on Tris or other ammonium salts, which exhibit a significant dependence of ionization constant on temperature. Tris buffer adjusted to pH of 8.3 at 25 °C decreases to pH 6.9 as temperature is raised to 95 °C. This pH change, however, has little effect on the stability of DNA duplexes (see Figure 1) as pK_Hs of the ionizable groups of the bases lie outside of this range. Nucleic acid−bases have pK_H values lower than 4.5 (dC) and greater than 9.4 (dG) in the single-stranded state which move even further from neutrality in the duplex state (*43*). Furthermore, the temperature range where primer hybridization and DNA synthesis occur during PCR is usually between 60 °C (the primer annealing step) and 72 °C (the enzymatic extension step). Within this narrow temperature window, pH varies only between 7.6 and 7.4. Thus the large pH shifts seen in Tris buffers with changes in temperature should have no effect on hybridization efficiency during PCR or other thermal cycling reactions. However, the protonated form of Tris is a monovalent cation and should be added to the total monovalent cation concentration when performing T_m calculations. Due to the relative extent of ionization, 10 mM Tris is equivalent to about 5 mM Na^+.

We have shown that the presence of dNTPs in a reaction mixture decreases the free magnesium ion concentration, which, in turn, lowers the T_m for DNA hybridization reactions done in that buffer. The Mg−dNTP association constant is sufficiently large (*50*) that the free Mg^{2+} concentration can be approximated simply by the difference between the total magnesium concentration and the total concentration of dNTPs. In a typical PCR reaction, the four dNTPs together are usually present at a concentration of 0.8 mM. Although sample DNA, primers and probes can also bind Mg^{2+}, their concentrations are too low to significantly affect the level of free Mg^{2+}.

During the course of PCR, dNTPs are consumed as DNA synthesis proceeds. However, this does not necessarily imply that free Mg^{2+} levels increase. Pyrophosphate, a byproduct of DNA synthesis, as well as the newly synthesized double-stranded DNA amplicon can also bind magnesium ions. We have not measured the fluctuations of free magnesium concentration during PCR.

ACKNOWLEDGMENT

The authors thank Drs. Isard Dunietz and Zhi-Jie Tan for helpful discussions on the stability of nucleic acid duplexes.

SUPPORTING INFORMATION AVAILABLE

Additional sets of T_m values used to develop and validate new magnesium correction, results of DSC and CD experiments, nearest-neighbor model of T_m magnesium correction and Δn calculations for duplexes that melt in non-two-state fashion. This material is available free of charge via the Internet at http://pubs.acs.org. Further, the database of average melting profiles, fraction of melted base pairs versus temperature, is available at http://biophysics.idtdna.com/Paper7/Abstract7.html.

REFERENCES

1. Sissoëff, I., Grisvard, J., and Guillé, E. (1976) Studies on metal ions-DNA interactions: specific behaviour of reiterative DNA sequences. *Prog. Biophys. Mol. Biol. 31*, 165–199.
2. Misra, V. K., and Draper, D. E. (1998) On the role of magnesium ions in RNA stability. *Biopolymers 48*, 113–135.
3. Saiki, R. K., Gelfand, D. H., Stoffel, S., Scharf, S. J., Higuchi, R., Horn, G. T., Mullis, K. B., and Erlich, H. A. (1988) Primer-directed enzymatic amplification of DNA with a thermostable DNA polymerase. *Science 239*, 487–491.
4. Hartwig, A. (2001) Role of magnesium in genomic stability. *Mutat. Res. 475*, 113–121.
5. Record, M. T., Jr (1975) Effects of Na^+ and Mg^{+2} ions on the helix-coil transition of DNA. *Biopolymers 14*, 2137–2158.
6. Korolev, N., Lyubartsev, A. P., and Nordenskiöld, L. (1998) Application of polyelectrolyte theories for analysis of DNA melting in the presence of Na^+ and Mg^{2+} ions. *Biophys. J. 75*, 3041–3056.
7. Tan, Z.-J., and Chen, S.-J. (2006) Nucleic acid helix stability: effects of salt concentration, cation valence and size, and chain length. *Biophys. J. 90*, 1175–1190.
8. Wilson, R. W., Rau, D. C., and Bloomfield, V. A. (1980) Comparison of polyelectrolyte theories of the binding of cations to DNA. *Biophys. J. 30*, 317–326.
9. Manning, G. S. (1972) On the application of polyelectrolyte "limiting laws" to the helix-coil transition of DNA. II. The effect of Mg^{+2} counterions. *Biopolymers 11*, 951–955.
10. Manning, G. S. (1978) The molecular theory of polyelectrolyte solutions with applications to the electrostatic properties of polynucleotides. *Q. Rev. Biophys. 11*, 179–246.
11. Olmsted, M. C., Anderson, C. F., and Record, M. T., Jr (1991) Importance of oligoelectrolyte end effects for the thermodynamics of conformational transitions of nucleic acid oligomers: a grand canonical Monte Carlo analysis. *Biopolymers 31*, 1593–1604.
12. Pack, G. R., Wong, L., and Lamm, G. (1999) Divalent cations and the electrostatic potential around DNA: Monte Carlo and Poisson-Boltzmann calculations. *Biopolymers 49*, 575–590.
13. Williams, A. P., Longfellow, C. E., Freier, S. M., Kierzek, R., and Turner, D. H. (1989) Laser temperature-jump, spectroscopic, and thermodynamic study of salt effects on duplex formation by dGCATGC. *Biochemistry 28*, 4283–4291.
14. Nakano, S., Fujimoto, M., Hara, H., and Sugimoto, N. (1999) Nucleic acid duplex stability: influence of base composition on cation effects. *Nucleic Acids Res. 27*, 2957–2965.
15. von Ahsen, N., Wittwer, C. T., and Schütz, E. (2001) Oligonucleotide melting temperatures under PCR conditions: nearest-neighbor corrections for Mg^{2+}, deoxynucleotide triphosphate, and dimethyl sulfoxide concentrations with comparison to alternative empirical formulas. *Clin. Chem. 47*, 1956–1961.
16. Peyret, N. (2000) Prediction of Nucleic Acid Hybridization: Parameters and Algorithms, Ph.D. Thesis, Section 5.4.2, pp 128, Wayne State University, Detroit, MI.
17. Dove, W. F., and Davidson, N. (1962) Cation effects on the denaturation of DNA. *J. Mol. Biol. 5*, 467–478.
18. Lyons, J. W., and Kotin, L. (1965) The effect of magnesium ion on the secondary structure of deoxyribonucleic acid. *J. Am. Chem. Soc. 87*, 1781–1785.
19. Ott, G. S., Ziegler, R., and Bauer, W. R. (1975) The DNA melting transition in aqueous magnesium salt solutions. *Biochemistry 14*, 3431–3438.
20. Krakauer, H. (1971) The binding of Mg^{+2} ions to polyadenylate, polyuridylate, and their complexes. *Biopolymers 10*, 2459–2490.
21. Krakauer, H. (1974) A thermodynamic analysis of the influence of simple mono- and divalent cations on conformational transitions of polynucleotide complexes. *Biochemistry 13*, 2579–2589.
22. Kankia, B. I. (2003) Binding of Mg^{2+} to single-stranded polynucleotides: hydration and optical studies. *Biophys. Chem. 104*, 643–654.
23. Draper, D. E. (2004) A guide to ions and RNA structure. *RNA 10*, 335–343.
24. Zubay, G., and Doty, P. (1958) Nucleic acid interactions with metal ions and amino acids. *Biochim. Biophys. Acta 29*, 47–58.
25. Rychlik, W., Spencer, W. J., and Rhoads, R. E. (1990) Optimization of the annealing temperature for DNA amplification in vitro. *Nucleic Acids Res. 18*, 6409–6412.
26. Harris, S., and Jones, D. B. (1997) Optimisation of the polymerase chain reaction. *Br. J. Biomed. Sci. 54*, 166–173.
27. Henegariu, O., Heerema, N. A., Dlouhy, S. R., Vance, G. H., and Vogt, P. H. (1997) Multiplex PCR: critical parameters and step-by-step protocol. *BioTechniques 23*, 504–511.
28. Markoulatos, P., Siafakas, N., and Moncany, M. (2002) Multiplex polymerase chain reaction: a practical approach. *J. Clin. Lab. Anal. 16*, 47–51.
29. Ignatov, K. B., Miroshnikov, A. I., and Kramarov, V. M. (2003) A new approach to enhanced PCR specificity. *Rus. J. Bioorg. Chem. 29*, 368–371.
30. Owczarzy, R., Vallone, P. M., Gallo, F. J., Paner, T. M., Lane, M. J., and Benight, A. S. (1997) Predicting sequence-dependent melting stability of short duplex DNA oligomers. *Biopolymers 44*, 217–239.
31. SantaLucia, J., Jr., and Hicks, D. (2004) The thermodynamics of DNA structural motifs. *Annu. Rev. Biophys. Biomol. Struct. 33*, 415–440.
32. Mitsuhashi, M. (1996) Technical Report: Part 1. Basic requirements for designing optimal oligonucleotide probe sequences. *J. Clin. Lab. Anal. 10*, 277–284.
33. Owczarzy, R., You, Y., Moreira, B. G., Manthey, J. A., Huang, L., Behlke, M. A., and Walder, J. A. (2004) Effects of sodium ions on DNA duplex oligomers: improved predictions of melting temperatures. *Biochemistry 43*, 3537–3554.
34. Moreira, B. G., You, Y., Behlke, M. A., and Owczarzy, R. (2005) Effects of fluorescent dyes, quenchers, and dangling ends on DNA duplex stability. *Biochem. Biophys. Res. Commun. 327*, 473–484.
35. Owczarzy, R. (2005) Melting temperatures of nucleic acids: discrepancies in analysis. *Biophys. Chem. 117*, 207–215.
36. Bevington, P. R., and Robinson, D. K. (1992) *Data Reduction and Error Analysis for the Physical Sciences*, WCB/McGraw-Hill, Boston, MA.
37. Press, W. H., Teukolsky, S. A., Vetterling, W. T., and Flannery, B. P. (1996) *Numerical Recipes in Fortran 77: The Art of Scientific Computing*, Cambridge University Press, Cambridge.
38. Good, N. E., Winget, G. D., Winter, W., Connolly, T. N., Izawa, S., and Singh, R. M. M. (1966) Hydrogen ion buffers for biological research. *Biochemistry 5*, 467–477.
39. Dawson, R. M. C., Elliot, D. C., Elliot, W. H., and Jones, K. M. (1986) *Data for Biochemical Research*, Oxford University Press, Oxford, U.K., pp 424.
40. Fukada, H., and Takahashi, K. (1998) Enthalpy and heat capacity changes for the proton dissociation of various buffer components in 0.1M potassium chloride. *Proteins 33*, 159–166.
41. Plum, G. E., and Breslauer, K. J. (1995) Thermodynamics of an intramolecular DNA triple helix: a calorimetric and spectroscopic study of pH and salt dependence of thermally induced structural transitions. *J. Mol. Biol. 248*, 679–695.
42. Privalov, P. L., and Ptitsyn, O. B. (1969) Determination of stability of the DNA double helix in an aqueous medium. *Biopolymers 8*, 559–571.
43. Record, M. T., Jr (1967) Electrostatic effects on polynucleotide transitions. II. Behavior of titrated systems. *Biopolymers 5*, 993–1008.
44. Gray, D. M. (1997) Derivation of nearest-neighbor properties from data on nucleic acid oligomers. I. Simple sets of independent sequences and the influence of absent nearest neighbors. *Biopolymers 42*, 783–793.

45. Schildkraut, C., and Lifson, S. (1965) Dependence of the melting temperature of DNA on salt concentration. *Biopolymers 3*, 195–208.
46. Tan, Z.-J., and Chen, S.-J. (2007) RNA helix stability in mixed Na^+/Mg^{2+} solution. *Biophys. J. 92*, 3615–3632.
47. Efron, B., and Tibshirani, R. J. (1993). *An Introduction to the Bootstrap*, Chapman & Hall/CRC, Boca Raton, FL.
48. Völker, J., Klump, H. H., Manning, G. S., and Breslauer, K. J. (2001) Counterion association with native and denatured nucleic acids: an experimental approach. *J. Mol. Biol. 310*, 1011–1025.
49. Philips, R. (1966) Adenosine and the adenine nucleotides. Ionization, metal complex formation, and conformation in solution. *Chem. Rev. 66*, 501–527.
50. Sigel, H. (1993) Interactions of metal ions with nucleotides and nucleic acids and their constituents. *Chem. Soc. Rev. 22*, 255–267.
51. Pecoraro, V. L., Hermes, J. D., and Cleland, W. W. (1984) Stability constants of Mg^{2+} and Cd^{2+} complexes of adenine nucleotides and thionucleotides and rate constants for formation and dissociation of MgATP and MgADP. *Biochemistry 23*, 5262–5271.
52. Hudson, R. H. E., Uddin, A. H., and Damha, M. J. (1995) Association of branched nucleic acids: structural and physicochemical analysis of antiparallel T•AT triple-helical DNA. *J. Am. Chem. Soc. 117*, 12470–12477.
53. Rose, D. M., Bleam, M. L., Record, M. T., Jr., and Bryant, R. G. (1980) ^{25}Mg NMR in DNA solutions: dominance of site binding effects. *Proc. Natl. Acad. Sci. U.S.A. 77*, 6289–6292.
54. Ma, C., and Bloomfield, V. A. (1995) Gel electrophoresis measurement of counterion condensation on DNA. *Biopolymers 35*, 211–216.
55. Cowan, J. A., Huang, H.-W., and Hsu, L. Y. (1993) Sequence selective coordination of Mg^{2+}(aq) to DNA. *J. Inorg. Biochem. 52*, 121–129.
56. Buckin, V. A., Kankiya, B. I., Rentzeperis, D., and Marky, L. A. (1994) Mg^{2+} recognizes the sequence of DNA through its hydration shell. *J. Am. Chem. Soc. 116*, 9423–9429.
57. Black, C. B., and Cowan, J. A. (1994) Quantitative evaluation of electrostatic and hydrogen-bonding contributions to metal cofactor binding to nucleic acids. *J. Am. Chem. Soc. 116*, 1174–1178.
58. Gessner, R. V., Quigley, G. J., Wang, A. H.-J., van der Marel, G. A., van Boom, J. H., and Rich, A. (1985) Structural basis for stabilization of Z-DNA by cobalt hexaammine and magnesium cations. *Biochemistry 24*, 237–240.
59. Sines, C. C., McFail-Isom, L., Howerton, S. B., VanDerveer, D., and Willimas, L. D. (2000) Cation mediate B-DNA conformational heterogeneity. *J. Am. Chem. Soc. 122*, 11048–11056.
60. Blagoi, Y. U. P., Sorokin, V. A., Valeyev, V. A., Khomenko, S. A., and Gladchenko, G. O. (1978) Magnesium ion effect on the helix-coil transition of DNA. *Biopolymers 17*, 1103–1118.
61. Anderson, C. F., and Record, M. T., Jr (1995) Salt-nucleic acid interactions. *Annu. Rev. Phys. Chem. 46*, 657–700.
62. Shkel, I. A., and Record, M. T., Jr (2004) Effect of the number of nucleic acid oligomer charges on the salt dependence of stability (ΔG°_{37}) and melting temperature (T_m): NLPB analysis of experimental data. *Biochemistry 43*, 7090–7101.
63. Elson, E. L., Scheffler, I. E., and Baldwin, R. L. (1970) Helix formation by d(TA) oligomers. III. Electrostatic effects. *J. Mol. Biol. 54*, 401–415.
64. Rouzina, I., and Bloomfield, V. A. (1997) Competitive electrostatic binding of charged ligands to polyelectrolytes: practical approach using the non-linear Poisson-Boltzmann equation. *Biophys. Chem. 64*, 139–155.
65. Bacquet, R. J., and Rossky, P. J. (1988) Ionic distributions and competitive association in DNA/mixed salt solutions. *J. Phys. Chem. 92*, 3604–3612.
66. SantaLucia, J., Jr (1998) A unified view of polymer, dumbbell, and oligonucleotide DNA nearest-neighbor thermodynamics. *Proc. Natl. Acad. Sci. U.S.A. 95*, 1460–1465.
67. Stellwagen, E., Dong, Q., and Stellwagen, N. C. (2007) Quantitative analysis of monovalent counterion binding to random-sequence, double-stranded DNA using the replacement ion method. *Biochemistry 46*, 2050–2058.
68. Bai, Y., Greenfeld, M., Travers, K. J., Chu, V. B., Lipfert, J., Doniach, S., and Herschlag, D. (2007) Quantitative and comprehensive decomposition of the ion atmosphere around nucleic acids. *J. Am. Chem. Soc. 129*, 14981–14988.

BI702363U